# Factors affecting B/Ca ratios in synthetic aragonite

M. Holcomb[1,2,3*], T.M. DeCarlo[4], G.A. Gaetani[5], M. McCulloch[1,2]

[1]The UWA Oceans Institute and School of Earth and Environment, The University of Western Australia, Crawley 6009, WA, Australia.

[2]ARC Centre of Excellence in Coral Reef Studies, The University of Western Australia, Crawley 6009, WA, Australia.

[3]Centre Scientifique de Monaco, Monaco, Principality of Monaco

[4]Massachusetts Institute of Technology/Woods Hole Oceanographic Institution Joint Program in Oceanography/Applied Ocean Physics and Department of Marine Geology and Geophysics, Woods Hole, MA 02543, U.S.A.

[5] Woods Hole Oceanographic Institution, Department of Marine Geology and Geophysics, Woods Hole, MA 02543, U.S.A.

*Corresponding author: mholcomb3051@gmail.com

Keywords: Boron; aragonite; coral; proxy; carbonate

**Abstract**

Measurements of B/Ca ratios in marine carbonates have been suggested to record seawater carbonate chemistry, however experimental calibration of such proxies based on inorganic partitioning remains limited. Here we conducted a series of synthetic aragonite precipitation experiments to evaluate the factors influencing the partitioning of B/Ca between aragonite and seawater. Our results indicate that the B/Ca ratio of synthetic aragonites depends primarily on the relative concentrations of borate and carbonate ions in the solution from which the aragonite precipitates; not on bicarbonate concentration as has been previously suggested. The influence of temperature was not significant over the range investigated (20 – 40 $^{o}$C), however, partitioning may be influenced by saturation state (and/or growth rate). Based on our experimental results, we suggest that aragonite B/Ca ratios can be utilized as a proxy of [$CO_3^{2-}$]. Boron isotopic composition ($\delta^{11}B$) is an established pH proxy, thus B/Ca and $\delta^{11}B$ together allow the full carbonate chemistry of the solution from which the aragonite precipitated to be calculated. To the extent that aragonite precipitation by marine organisms is affected by seawater chemistry, B/Ca may also prove useful in reconstructing seawater chemistry. A simplified boron purification protocol based on amberlite resin and the organic buffer TRIS is also described.

## 1. Introduction

Boron concentrations and boron isotopic compositions in marine carbonates are potential archives of past seawater pH and carbonate chemistry (e.g. Sanyal et al., 1996; Pelejero et al., 2005; Pearson and Palmer, 1999; Douville et al., 2010; Rae et al., 2011; Henehan et al., 2013; Penman et al., 2013). In seawater, boron is typically present in

45 two forms, boric acid ($B(OH)_3$) and borate ($B(OH)_4^-$), the relative abundances of which
46 depend largely on pH (e.g. Culberson, 1968; Dickson, 1990; Klochko et al., 2006). The
47 $B(OH)_4^-$ ion is thought to be the primary form of boron incorporated into calcium
48 carbonate (e.g. Sen et al., 1994; Hemming et al., 1995), thus offering the potential to use
49 B/Ca ratios to estimate pH and/or carbonate chemistry (e.g. Yu et al., 2007). However,
50 there is uncertainty as to how boron incorporation may depend upon concentrations of
51 different dissolved inorganic carbon (DIC) species (e.g. Hemming et al., 1995; Uchikawa
52 et al., 2015). In addition, there are suggestions that $B(OH)_3$ may also be incorporated,
53 especially in calcite (e.g. Xiao et al., 2008; Klochko et al., 2009; Rollion-Bard et al.,
54 2011; Mavromatis et al., 2015; Uchikawa et al., 2015), thus potentially complicating the
55 interpretation of B/Ca ratios.
56 Various relationships have been used to explore the range of possible factors
57 controlling B incorporation in both synthetic (e.g. Mavromatis et al., 2015; Uchikawa et
58 al., 2015) and biogenic carbonates (e.g. Ni et al., 2007; Yu et al., 2007; Yu and
59 Elderfield, 2007; Foster 2008; Douville et al., 2010; Allen et al., 2011; Rae et al., 2011;
60 Tripati et al., 2011; Allen et al., 2012; Allison et al., 2014; Babila et al., 2014; Henehan et
61 al., 2015). Here we consider several of the relationships proposed by previous studies:
62 $B(OH)_4^-/CO_3^{2-}$, $B(OH)_4^-/HCO_3^-$, $B(OH)_4^-/(CO_3^{2-} + HCO_3^-)$, $B/HCO_3^-$, $B/(CO_3^{2-} + HCO_3^-)$,
63 $B(OH)_4^-/\Delta CO_3^{2-}$ (where $\Delta CO_3^{2-}$ is the difference between the actual $[CO_3^{2-}]$ and the
64 $[CO_3^{2-}]$ at which the solution would be saturated with respect to aragonite, $\Omega_{Arag} = 1$). In
65 addition to various empirical relationships, we also consider potential balanced exchange
66 reactions with the following expressions for the distribution coefficient:
67

reaction 1 (Hemming and Hanson 1992):

$CaCO_3 + B(OH)_4^- \leftrightarrow Ca(HBO_3) + HCO_3^- + H_2O$

$$K_D = \frac{[HBO_3^{2-} / CO_3^{2-}]_{CaCO_3}}{[B(OH)_4^- / HCO_3^-]_{solution}} \quad \text{eq. 1}$$

reaction 2: $0.5\ CaCO_3 + B(OH)_4^- \leftrightarrow Ca_{0.5}B(OH)_4 + 0.5\ CO_3^{2-}$

$$K_D = \frac{[B(OH)_4^- / [CO_3^{2-}]^{0.5}]_{CaCO_3}}{[B(OH)_4^- / [CO_3^{2-}]^{0.5}]_{solution}} \quad \text{eq. 2}$$

reaction 3: $3\ CaCO_3 + 2\ B(OH)_4^- \leftrightarrow Ca_3(BO_3)_2 + CO_2 + 2\ HCO_3^- + 3\ H_2O$

$$K_D = \frac{[[BO_3^{3-}]^2 / [CO_3^{2-}]^3]_{CaCO_3}}{[[B(OH)_4^-]^2 / [CO_2][HCO_3^-]^2]_{solution}} \quad \text{eq. 3}$$

Studies of naturally formed samples do provide some insights into the potential controls on boron incorporation (Hemming and Hanson 1992; Sanyal et al., 1996; Wara et al., 2003; Ni et al., 2007; Yu et al., 2007; Yu and Elderfield, 2007; Foster et al., 2008; Rollion-Bard et al., 2011; Allison et al., 2014; Kaczmarek et al., 2015). However, such studies cannot establish how B/Ca is controlled by environmental variables due to inevitable uncertainty as to the conditions during carbonate deposition. This is particularly the case for calcifying organisms that modify the conditions at the site of calcification substantially from the conditions present in the surrounding seawater (e.g. Al-Horani et al., 2003; McCulloch et al., 2012; De Nooijer et al., 2014). Since the chemistry at the site of calcification is generally unknown, most studies have focused on the relationship between B/Ca and seawater chemistry. Thus in studies of biologically

88 formed calcium carbonate, there is uncertainty as to whether B/Ca changes in direct
89 response to environmental conditions, or if it reflects physiological changes in the
90 organism.

91 Laboratory studies on the incorporation of B into calcium carbonate remain
92 limited, and few potentially controlling factors (e.g. temperature, carbonate chemistry,
93 growth rate etc) have been tested (Kitano et al., 1978; Sen et al. 1994; Hemming et al.,
94 1995; Hobbs and Reardon, 1999; Sanyal et al., 2000; Xiao et al., 2008; He et al., 2013;
95 Gabitov et al., 2014; Mavromatis et al., 2015; Uchikawa et al., 2015). Critically only one
96 study has characterized the carbonate chemistry during aragonite precipitation
97 (Mavromatis et al., 2015).

98 We conducted a series of experiments to explore how carbonate chemistry,
99 organic additives, temperature, and boron concentration may influence B/Ca ratios in
100 aragonite formed from seawater-like solutions. Manipulation of pH, DIC, and $Ca^{2+}$ are
101 among the mechanisms potentially driving biogenic calcification, thus our experiments
102 focused on manipulating these variables. In addition to these inorganic variables, there
103 are also a wide range of organic molecules produced by calcifying organisms which may
104 influence calcification (e.g. Mass et al., 2013). We chose to test one specific mechanism
105 by which organic molecules could influence B/Ca, that of buffering pH. In seawater, the
106 two dominant pH buffers are DIC and B species, thus variations in pH (such as might
107 occur adjacent to a growing aragonite crystal) would directly affect DIC and B
108 speciation. By adding an additional buffering agent (such as 2-Amino-2-hydroxymethyl-
109 propane-1,3-diol (TRIS) or 4-(2-hydroxyethyl)-1-piperazineethanesulfonic acid
110 (HEPES)), pH could in theory be more stable adjacent to the growing crystal which could

111 alter the relationship between B/Ca and bulk solution chemistry. In addition to biological
112 processes affecting elemental ratios, there is also a potential for some of the compounds
113 used to study crystal growth to influence elemental incorporation. Calcein is among the
114 molecules commonly used to mark growing crystals in living organisms (e.g. Venn et al.,
115 2013), and the influence of calcein on the incorporation of a number of elements has been
116 tested (Dissard et al., 2009), though no information is thus-far available as the effect of
117 calcein on B/Ca, thus it was tested here.
118
119 **2. Methods**
120 *2.1. Aragonite precipitation*
121 Aragonite was precipitated from seawater (0.2 μm filtered to remove living
122 organisms) using several different approaches adapted from existing methods (Kinsman
123 and Holland 1969; Kitano et al., 1978; Gaetani and Cohen 2006; Holcomb et al., 2009;
124 Gabitov et al., 2011; Wang et al., 2013). The range of experimental protocols used was
125 intended to precipitate aragonite under a wide range of solution chemistries in order to
126 encompass the likely compositional range of biologically mediated solutions and thus
127 more fully evaluate the factors that affect boron incorporation during bio-calcification.
128 Detailed descriptions of the protocols used for each of the 65 experiments are provided in
129 the supplementary materials (see section S1 and Table S1 for more details). Briefly, all
130 experiments were carried out in plastic containers held within constant temperature water
131 baths. Two general types of experiments were conducted: degassing (Figure 1B) and
132 pumping (Figure 1A) experiments. Degassing experiments were carried out by
133 dissolving $CaCO_3$ in seawater at ~1 atm $pCO_2$ with the addition of $MgCl_2$, $SrCO_3$ (to

maintain seawater like Mg/Ca and Sr/Ca ratios) and various additives (TRIS, HEPES, calcein, boron, $CaCl_2$, etc. depending upon the experiment). As $CO_2$ degassed in these experiments, $\Omega_{Arag}$ increased until aragonite began to precipitate. Degassing experiments were bubbled at controlled rates with air or air/$CO_2$ mixes during precipitation to stabilize pH. Pumping experiments were conducted by adding seawater containing $CaCO_3$ (dissolved by bubbling with $CO_2$) or concentrated seawater (evaporated to achieve 2x normal salinity = 2xsw) and a $NaHCO_3$ or $Na_2CO_3$ or NaOH or mixture there-of solution (here after referred to as NaX solution) to seawater using a syringe pump. The simultaneous injection of 2xsw and NaX solutions allowed carbonate chemistry to be modified while maintaining salinity ~constant. Pumping rates were varied over the course of each experiment to stabilize pH during precipitation. Some of these experiments were additionally bubbled with air or air/$CO_2$ mixtures, and some contained additional additives. All experiments were stirred continuously.

The evolution of solution chemistry during precipitation differed among experiments. In general, in pumping experiments an initial pH and alkalinity was established, precipitation then removed $CO_3^{2-}$ thus reducing DIC (or equivalently total inorganic carbon) and alkalinity, while pumping of the NaX solution added DIC and alkalinity, thus allowing carbonate chemistry to be maintained nearly constant during precipitation. In degassing experiments, though pH was maintained nearly constant, DIC, and alkalinity both declined during precipitation due to the precipitate removing DIC and alkalinity and bubbling removing DIC. To illustrate the relationships between different solution chemistry parameters potentially relevant for B/Ca, Figure 2 shows

156 various chemical parameters plotted versus $pH_T$ for our experiments, as well as the values
157 expected for seawater at different DIC concentrations.
158

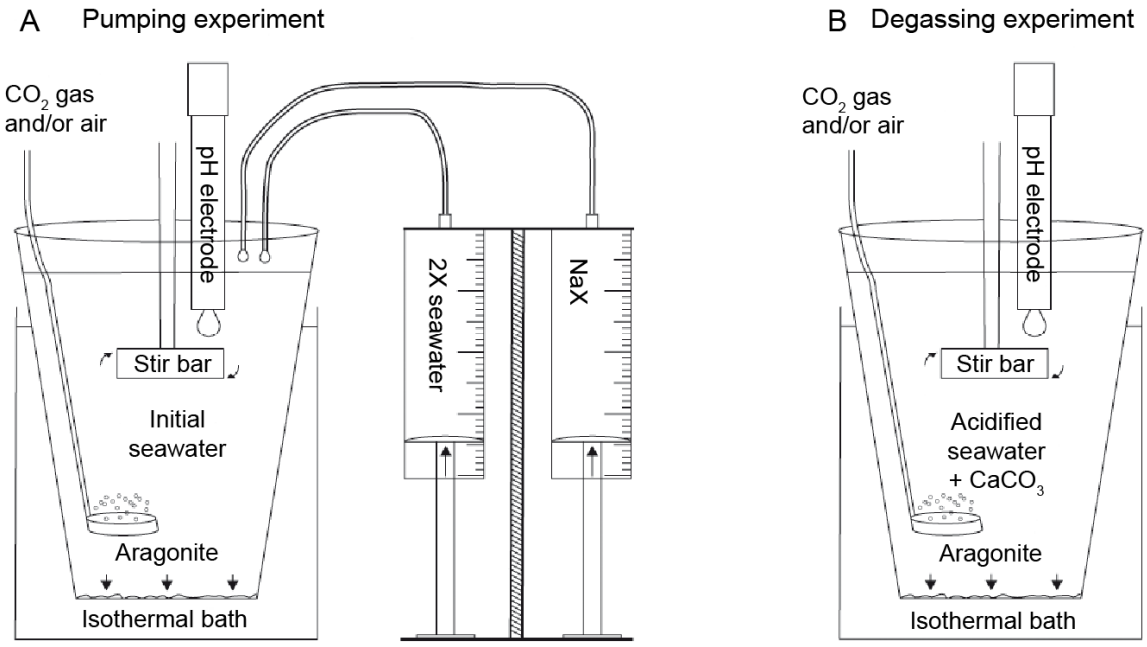


159

160 Figure 1. Schematic representation of the experimental setup used for pumping (A) and
161 degassing (B) experiments.

Over the course of each experiment, samples were taken for pH, alkalinity, and solution chemistry measurements. Samples for alkalinity and solution chemistry were filtered (Millex-HV syringe filter, 0.45 μm PVDF membrane) at the time of collection to remove any aragonite particles potentially present. All seawater samples used for elemental composition measurements were acidified with concentrated $HNO_3$ to dissolve any material that precipitated post-collection. Details of all measurements, associated calculations, and measured values are provided in the supplementary materials (sections S2, S3, and .xls file).

### *2.2. Precipitate Characterization*

#### *2.2.1. Mineralogy*

The mineralogy of most experiments was characterized by XRD (see supplemental materials section S4) and/or Raman spectroscopy (DeCarlo et al., 2015; and supplemental materials S4). Some experiments contained phases other than aragonite and were generally excluded from analysis of B/Ca, with the exception of one sample (10h) which had a faint XRD peak near 2-theta = 30, suggesting possible contamination with a calcitic phase, but neither the Raman spectra nor the elemental composition indicated a non-aragonitic phase, thus any contamination was assumed to be sufficiently low as to not compromise the use of the sample.

#### *2.2.2. Composition*

184 The elemental composition of all precipitates was measured using Q-ICPMS
185 (supplemental materials S3.1) to verify that the elemental composition was similar to
186 other marine aragonite samples while simultaneously measuring the B/Ca ratio. The
187 coral standard JCp-1 (B/Ca = 0.4596 mmol $mol^{-1}$, Hathorne et al. (2013)) was used to
188 standardize all measurements, and the validity of this approach for measuring B/Ca was
189 verified using independent measurements of purified boron extracts measured via MC-
190 ICPMS (supplemental materials S3.2.1). Data on the incorporation of Sr/Ca and U/Ca
191 into these precipitates is published elsewhere (DeCarlo et al., 2015).
192
193 *2.3. Solution Characterization*
194 Since natural seawater was used for all experiments, and Ca and B are generally
195 considered uniformly distributed throughout the oceans in proportion to salinity,
196 concentrations were calculated based on salinity and the mass of any added B- or Ca-
197 containing solutions. For a subset of experiments the validity of this assumption was
198 verified via ICP-MS measurements. Measurements are described in the supplemental
199 materials including the description of new simplified chemistry for the purification of
200 boron based on amberlite IRA 743 resin and the organic buffer TRIS (supplemental
201 material S3.3).
202
203 *2.4. Calculations*
204 Carbonate chemistry was calculated using the measured alkalinity, pH, and temperature.
205 When pH measurements were carried out at a temperature different from that of the
206 experimental temperature, the pH at the experimental temperature was calculated using

CO2Sys (van Heuven et al., 2009). Salinities were interpolated based on initial and final salinities and estimated evaporation rates. Calcium and boron concentrations in the fluid were calculated based on salinity, estimated amount of precipitate deposited, and any calcium or boron added to the experiment. These experiments were undertaken in conjunction with those reported by DeCarlo et al. (2015), further details are given in the supplemental materials (S2), as are alternative calculations using constants from Hain et al. (2015) (S6).

Since aragonite is primarily $CaCO_3$, and thus $Ca \approx CO_3$, B/Ca can be substituted for $B/CO_3$ when calculating distribution coefficients, so though equations 1-3 are expressed relative to $CO_3$ in the solid, B/Ca will be used for calculations.

*2.5. Average solution chemistry and partitioning*

We evaluated the factors controlling B incorporation into aragonite by comparing the bulk/mean aragonite B/Ca ratio to the average solution composition during precipitation of each of 58 experiments conducted in 2013 (of 65 total experiments). The solution chemistry and bulk precipitation rates varied over the course of each experiment. To estimate the average solution chemistry during the time that aragonite precipitated, chemistry parameters were weighted by the amount of precipitate formed over the given time interval (estimated from the difference between measured and expected alkalinity). The distribution coefficient relationship that best described the data was then used to calculate distribution coefficients for each individual experiment such that the calculated B/Ca ratio for the final precipitate in each experiment matched the measured ratio. Data from experiments run in 2011 (denoted by a '/11' in the experiment name in the

230 supplemental tables) were not included in these comparisons as carbonate chemistry was
231 generally less stable; experiments from 2011 were used only for assessing the effects of
232 calcein.
233
234 ***3. Results***
235 Aragonite was precipitated over a wide range of $pH_T$ (7.3 to 9.3, where $pH_T$ is pH
236 measured on the total scale), temperature (~20 $^oC$ to 40 $^oC$), and carbonate chemistry
237 conditions (Fig. 2). Within any given experiment, the precipitate formed under a range of
238 solution chemistry conditions, but the range within an experiment was generally small
239 relative to the differences among experiments (Fig. 2). For example, the within-
240 experiment pH variation was typically less than 0.1 pH units, whereas among
241 experiments pH differences of more than 2 pH units were achieved. Likewise, within the
242 course of an experiment, the relative standard deviation (RSD) of $[B(OH)_4^-]/[CO_3^{2-}]^{0.5}$
243 was less than 15% (typically less than 5%), while different experiments differed by more
244 than an order of magnitude (Figure 2H, Table S2).
245 The B/Ca ratio in the precipitate showed no significant ($p > 0.05$) correlation with $pH_T$ or
246 any single carbonate chemistry parameter. Significant ($p < 0.001$) correlations were
247 found between B/Ca and the mean solution [B] and $[B(OH)_4^-]$ (Table 1). However, when
248 considering only precipitates formed under seawater boron concentrations, B/Ca does
249 correlate significantly with a number of carbonate system parameters, most notably pH
250 and parameters closely correlated with pH (e.g. DIC species and $[B(OH)_4^-]$; Figure 3,
251 Table 1), with $[B(OH)_4^-]$ remaining the single parameter most strongly correlated with
252 B/Ca.

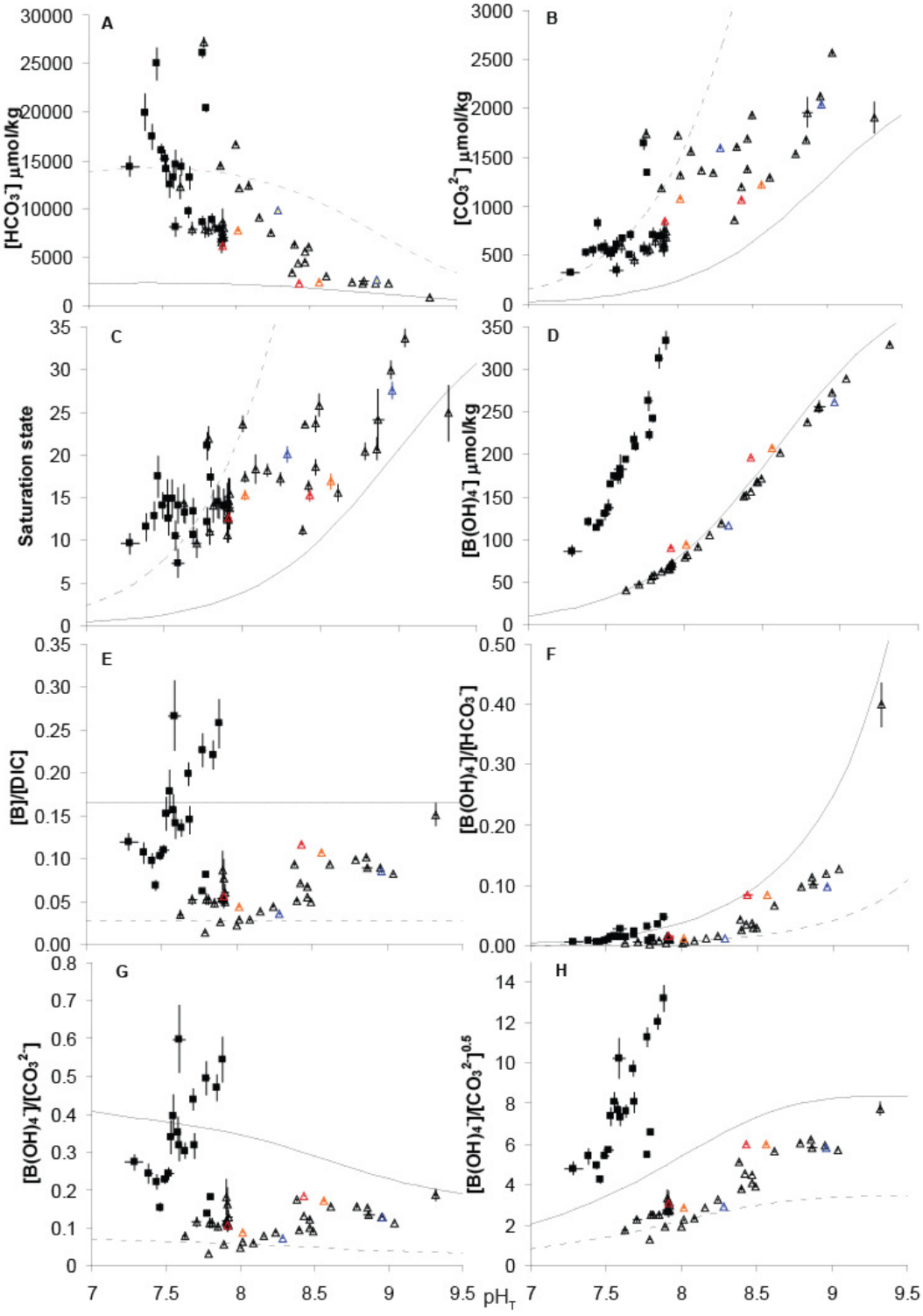
A
B
C
D
E
F
G
H
[HCO3-] µmol/kg
[CO3 2-] µmol/kg
Saturation state
[B(OH)4-] µmol/kg
[B]/[DIC]
[B(OH)4-]/[HCO3-]
[B(OH)4-]/[CO3 2-]
[B(OH)4-]/[CO3 2-]0.5
pHT

Figure 2. Relationship between different solution chemistry parameters and $pH_T$ (total scale pH) Symbols are means of individual experiments; experiments without added B are represented by triangles, experiments with added B are represented by squares, lines show bi-direction error bars (1 standard deviation (sd)). Experiments conducted at different temperatures are shown in different colors: blue ~ 20, black ~ 25, orange ~ 33, and red ~ 40 $^{o}$C. Most experiments were conducted at ~ 25 $^{o}$C, 2 experiments were run at each of the other temperatures. Lines show calculated concentrations of different DIC species and borate (µmol/kg sw) as a function of seawater $pH_T$. Calculated values are for seawater (S=35, T=25 $^{o}$C) with either 2500 (solid line) or 15000 (dashed line) µmol DIC/kg sw.

Table 1. Pearson correlation coefficients for mean solution chemistry parameters showing the most significant correlations with the B/Ca ratio of the precipitate, as well as various proposed ratios suggested to be linked to B/Ca regardless of significance. Correlation coefficients are given for the data set as a whole (n=58, excluding experiments run in 2011), for experiments without added B (n=39), and for pumping experiments without added B (n=28). Significant ($p<0.05$) individual correlations are indicated by $^{*}$.

| Species in solution | Correlation with precipitate B/Ca | | |
|---|---|---|---|
| | All experiments | Experiments with seawater [B] | Pumping experiments with seawater [B] |
| $pH_T$ | 0.03 | 0.80$^{*}$ | 0.81$^{*}$ |
| $[HCO3^-]$ | -0.16 | -0.80$^{*}$ | -0.81$^{*}$ |
| DIC | -0.18 | -0.77$^{*}$ | -0.80$^{*}$ |
| $[B(OH)_4^-]^2 /[CO_2][HCO_3^-]^2$ | 0.19 | 0.46$^{*}$ | 0.47$^{*}$ |
| $[B(OH)_4^-]/[HCO_3^-]$ | 0.33$^{*}$ | 0.77$^{*}$ | 0.76$^{*}$ |
| $[B(OH)_4^-]/([CO_3^{2-}] + [HCO_3^-])$ | 0.47$^{*}$ | 0.90$^{*}$ | 0.90$^{*}$ |
| $[B(OH)_3]$ | 0.55$^{*}$ | -0.82$^{*}$ | -0.83$^{*}$ |
| [B]/[Ca] | 0.58$^{*}$ | 0.38$^{*}$ | 0.23 |
| [B] | 0.62$^{*}$ | -0.41$^{*}$ | -0.35 |
| $[B(OH)_4^-]/\Delta CO_3^{2-}$ | 0.78$^{*}$ | 0.70$^{*}$ | 0.92$^{*}$ |
| $[B(OH)_4^-]$ | 0.79$^{*}$ | 0.82$^{*}$ | 0.83$^{*}$ |
| $[B]/[HCO_3^-]$ | 0.81$^{*}$ | 0.84$^{*}$ | 0.85$^{*}$ |
| $[B(OH)_4^-]/[CO_3^{2-}]$ | 0.83$^{*}$ | 0.81$^{*}$ | 0.93$^{*}$ |
| $[B]/([CO_3^{2-}] + [HCO_3^-])$ | 0.89$^{*}$ | 0.93$^{*}$ | 0.97$^{*}$ |
| [B]/[DIC] | 0.89$^{*}$ | 0.94$^{*}$ | 0.97$^{*}$ |
| $[B(OH)_4^-]*[Ca^{2+}]$ | 0.92$^{*}$ | 0.82$^{*}$ | 0.81$^{*}$ |
| $[B(OH)_4^-]/[CO_3^{2-}]^{0.5}$ | 0.95$^{*}$ | 0.94$^{*}$ | 0.95$^{*}$ |

Since boron is thought to compete with DIC species for incorporation into aragonite (e.g. Hemming et al., 1992), correlations between precipitate B/Ca and various solution

277 boron/DIC relationships were explored (Table 1). In the full data-set, B/Ca and mean
278 $[B(OH)_4^-]/[HCO_3^-]$ were not strongly correlated (Fig. 3b, based on equation 1), nor were
279 the residuals of a $[B(OH)_4^-]$ vs B/Ca regression and $[HCO_3^-]$. Nor was there a significant
280 correlation between B/Ca and average $[B(OH)_4^-]^2/[CO_2][HCO_3^-]^2$ (equation 3). B/Ca in
281 the precipitate was most strongly correlated with the mean $[B(OH)_4^-]/[CO_3^{2-}]^{0.5}$ (equation
282 2), [B]/[DIC] or $[B]/([CO_3^{2-}] + [HCO_3^-])$ and $[B(OH)_4^-]*[Ca^{2+}]$ (Table 1, Fig. 3). The
283 correlations of B/Ca with $[B(OH)_4^-]/[CO_3^{2-}]^{0.5}$ and [B]/[DIC] or $[B]/([CO_3^{2-}] + [HCO_3^-])$
284 were important regardless of whether B was added or whether only pumping or degassing
285 experiments were considered. Conversely $[B(OH)_4^-]*[Ca^{2+}]$, though significantly
286 correlated with B/Ca, did not necessarily correlate more strongly than $[B(OH)_4^-]$ alone
287 (Table 1). When only a subset of the experiments is considered, some of the other
288 potential relationships become significant (Table 1). For instance, $[B(OH)_4^-]/[CO_3^{2-}]$ is
289 highly correlated with B/Ca, especially for pumping experiments, as is $[B(OH)_4^-]/[CO_3^{2-}]^{0.5}$, yet these two ratios show opposite behaviors in seawater as a function of pH (Fig.
291 2G,H). Given the range of DIC (2.8 – 29 mmol/kg sw) and [B] (0.39 – 2.1 mmol/kg sw)
292 among experiments (Table S2), DIC and [B] would be expected to have a greater
293 influence on $[B(OH)_4^-]/[CO_3^{2-}]$ and $[B(OH)_4^-]/[CO_3^{2-}]^{0.5}$ than pH, thus a positive
294 correlation is expected. Similarly mean $[B(OH)_4^-]/[CO_3^{2-}]^{0.5}$ and [B]/[DIC] were highly
295 correlated (Pearson correlation coefficient: 0.954) as would be expected given the large
296 ranges of DIC and [B] and their consequent influence on $[B(OH)_4^-]/[CO_3^{2-}]^{0.5}$ (e.g. Fig.
297 2). Since DIC is nearly equivalent to $[CO_3^{2-}] + [HCO_3^-]$, no separate treatment will be
298 given of the $[B]/([CO_3^{2-}] + [HCO_3^-])$ relationship. Linear least squares regression
299 (excluding one outlier, experiment 1c) gave the following fits:

B/Ca (mmol/mol) = .0604 (±0.0022) $[B(OH)_4^-]/[CO_3^{2-}]^{0.5}$ +.0411 (±0.012) eq. 4

B/Ca (mmol/mol) = 2.88 (±0.13) [B]/[DIC] + 0.085 (±0.014) eq. 5

where $[B(OH)_4^-]$, $[CO_3^{2-}]$, [B], and [DIC] are in units of μmol kg $sw^{-1}$, values in parentheses are 1 standard error, all parameter estimates were significant ($p \leq 0.001$, $R^2$=0.93 for eq. 4, $R^2$=0.89 for eq. 5).

Although our data provide no means of assessing whether B/Ca in the aragonite precipitate depends upon solution $[B(OH)_4^-]/[CO_3^{2-}]^{0.5}$ or [B]/[DIC], the relationship based on borate and carbonate was chosen for further investigation as $CO_3^{2-}$ was considered to be more relevant for precipitation than total DIC (see supplemental section S6 for calculations based on DIC as well as $Ca^{2+}$).

Within any given experiment, the precipitate formed under a range of solution chemistry conditions. However, the range within an experiment was generally small relative to the differences among experiments. Thus $K_D$ was assumed to be constant for a given experiment allowing $K_D$ values to be calculated for each individual experiment *i*:

$$\frac{B_i}{Ca_i} = \frac{B_i}{(CO_3)_i^{0.5}} = K_{D_i} \times \sum_{j=1}^{j=n} \frac{[B(OH)_4^-]_{i,j} \times w_{i,j}}{[CO_3^{2-}]_{i,j}^{0.5}}$$

Where B/Ca is measured and is in mmol/mol, $[B(OH)_4^-]$ and $[CO_3^{2-}]$ are in units of μmol kg $sw^{-1}$, *w* is the fraction of total aragonite formed in time interval *j* as estimated from the difference in expected and measured alkalinity, *i* signifies an individual experiment, and *j* is one of *n* measurements taken during the course of aragonite precipitation in experiment

322 *i*. Aragonite is assumed to be pure $CaCO_3$, thus Ca = $CO_3$ with activities = 1, so the
323 exponent can be dropped for the solid phase. Calculated $K_D$ values ranged from 0.042-
324 0.103, with an average of 0.071 +/- 0.011 sd. $K_D$ values were correlated with a number
325 of solution chemistry parameters (Fig. S4), but regressions with [B] and either $[CO_3^{2-}]$ or
326 saturation state with respect to aragonite ($\Omega$) explained much of the variance:
327
328 $K_D = -0.0109\ (\pm 0.00157)\ [B] - 0.001106\ (\pm 0.00021)\ \Omega + 0.0994\ (\pm 0.00432)$ eq. 6
329
330 $K_D = -0.01215\ (\pm 0.00159)\ [B] - 0.0000119\ (\pm 0.000002)\ [CO_3^{2-}] + 0.09474\ (\pm 0.00323)$
331 eq. 7
332 where [B] is in units of mmol kg $sw^{-1}$, and $[CO_3^{2-}]$ is in units of μmol kg $sw^{-1}$, with
333 $R^2$=0.49, p<0.001 and $R^2$=0.53, p<0.001 for equation 6 and 7 respectively. Note that
334 $\Omega$ and $[CO_3^{2-}]$ were highly correlated (Pearson correlation coefficient: 0.94).
335 Using eqs. 6-7, the B/Ca ratio for each precipitate was predicted based on each
336 measurement time-point. The differences between the measured and predicted B/Ca
337 ratios showed no significant correlation with any solution chemistry parameter (see
338 supplemental .xls file), nor was there any significant effect of temperature, calcein, nor of
339 organic buffering compounds (though precipitates formed in the presence of HEPES
340 tended to have B/Ca ratios higher than predicted, while those formed in the presence of
341 TRIS tended to be lower). Differences between measured and predicted (for both
342 equations 6 and 7) B/Ca ratios were typically less than 0.03 mmol/mol or 8% relative
343 difference.

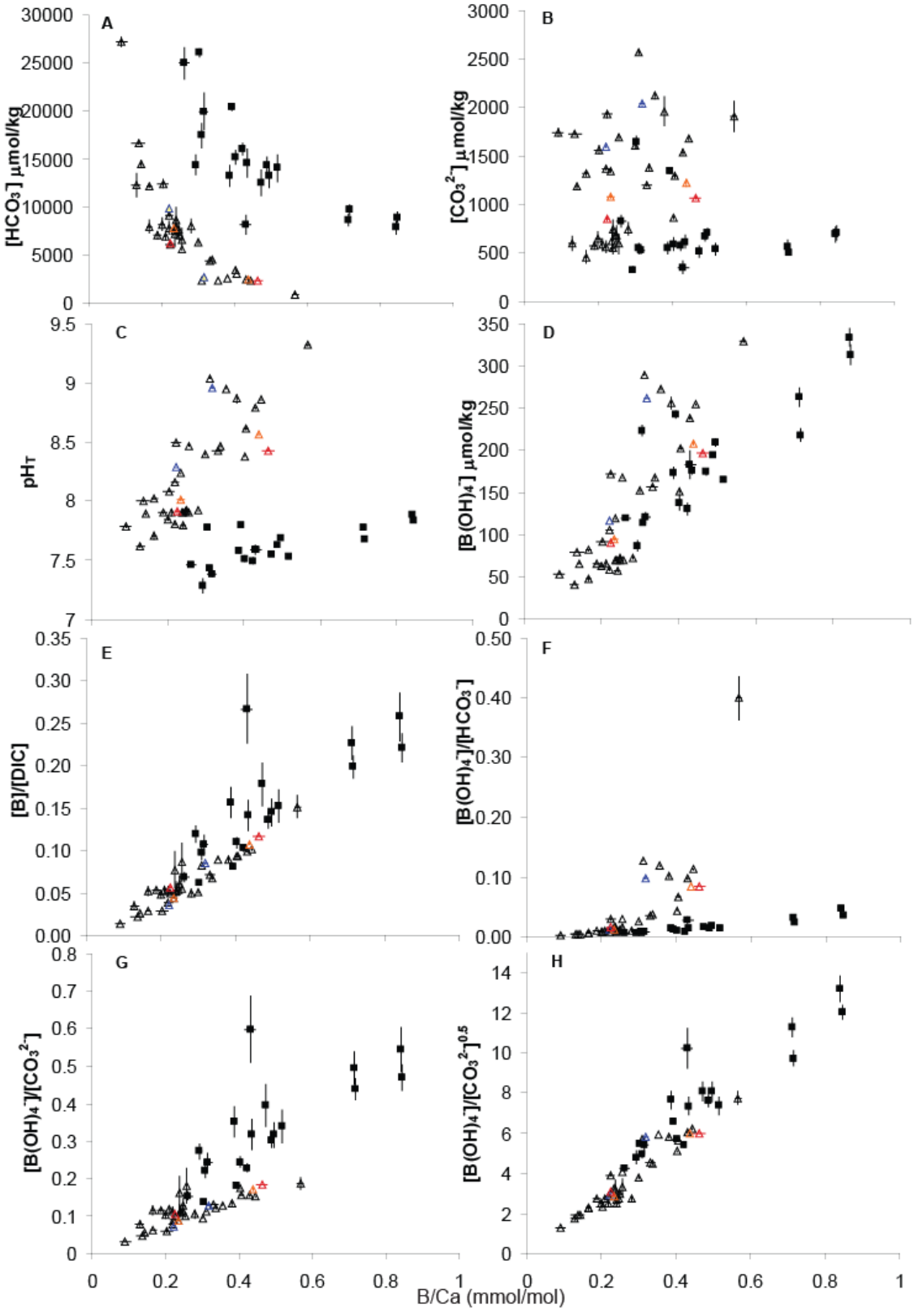
A
B
C
D
E
F
G
H
[HCO3] µmol/kg
[CO3 2] µmol/kg
pHT
[B(OH)4] µmol/kg
[B]/[DIC]
[B(OH)4]/[HCO3]
[B(OH)4]/[CO3 2]
[B(OH)4]/[CO3 2]0.5
B/Ca (mmol/mol)

346 Figure 3. Relationship between B/Ca (mmol/mol) in aragonite and various solution
347 chemistry parameters. Units for all species in solution are μmol/kg sw. Symbols are as
348 described for figure 2.

## *4. Discussion*

How boron is incorporated into aragonite remains uncertain. Many relationships (e.g. Eqs. 1-3) have been proposed to explain how B/Ca depends on solution chemistry. The wide range of solution chemistries achieved in our experiments allows us to evaluate many of the proposed relationships.

In contrast to previous work (Hemming and Hanson, 1992), we found no significant relationship between the B/Ca ratio in aragonite and the $[B(OH)_4^-]/[HCO_3^-]$ ratio in solution (Fig. 3f). Rather, our results indicate that B/Ca depends on $[B(OH)_4^-]/[CO_3^{2-}]^{0.5}$ (Fig. 3h), suggesting that equation 2 represents the appropriate expression for the distribution coefficient. A dependence of B/Ca on $[B(OH)_4^-]$ and $[CO_3^{2-}]$ is the most likely scenario, due both to data suggesting $B(OH)_4^-$ to be the primary form of B incorporated (e.g. Hemming et al., 1995; Mavromatis et al., 2015), and the involvement of $CO_3^{2-}$ in the formation of $CaCO_3$ (but see Wolthers et al., 2012). For a reaction involving $B(OH)_4^-$ and $CO_3^{2-}$, a $B(OH)_4^-$ can balance the charge of only ½ a $CO_3^{2-}$, thus a dependence on $[B(OH)_4^-]/[CO_3^{2-}]^{0.5}$ would be expected, consistent with our data (Fig. 3D).

Other possibilities do, however, exist. The significant correlation between B/Ca and $[B(OH)_4^-]*[Ca^{2+}]$ could suggest the involvement of $CaB(OH_4)^+$, though it could also reflect the importance of $[B(OH)_4^-]$ combined with a negative correlation between $[CO_3^{2-}]$ and [Ca] in a sub-set of experiments (discussed further in the supplement). Variations in [B]/[DIC] were strongly correlated with B/Ca and $[B(OH)_4^-]/[CO_3^{2-}]^{0.5}$ reflecting the dependence of $[B(OH)_4^-]/[CO_3^{2-}]^{0.5}$ on [B] and [DIC] combined with the pH dependencies of both B and DIC species; thus we cannot rule out the possibility of B/Ca

372 being controlled by [B]/[DIC]. For calcite, existing work points to [B]/[DIC] and growth
373 rate being the primary controls on B/Ca (Uchikawa et al., 2015). However, recalculating
374 the data of Uchikawa et al. (2015) as B/Ca / $[B(OH)_4^-]/[CO_3^{2-}]^{0.5}$ versus growth rate gives
375 a very similar fit to that obtained with [B]/[DIC] ($R^2$=0.86 vs 0.88), again reflecting the
376 difficulty of experimentally decoupling these parameters without simultaneously
377 changing other chemical parameters.
378
379 *4.1. Partition coefficient $K_D$*
380 Using our experimental data, we calculated partition coefficients ($K_D$) for $[B(OH)_4^-$
381 $]/[CO_3^{2-}]^{0.5}$ between aragonite and solution. This allows us to identify which factors
382 influence B/Ca ratios in addition to the primary control of the solution $[B(OH)_4^-]/[CO_3^{2-}$
383 $]^{0.5}$ ratio. The $K_D$ appears to depend upon the boron concentration and the saturation state
384 or $[CO_3^{2-}]$ (equation 6, 7, Fig. S4). A dependence upon boron concentration is consistent
385 with previous work (Hemming et al., 1995), though our experiments likely did not cover
386 a large enough range of [B] to fully describe this dependence (discussed below). In
387 addition, we found a relationship between $K_D$ and saturation state, which may reflect the
388 influence of growth rate because aragonite crystals precipitate faster from solutions of
389 greater supersaturation (e.g. Burton and Walter 1987). Other studies have also suggested
390 a growth rate influence on boron incorporation in calcite (Hobbs and Reardon, 1999;
391 Gabitov et al., 2014; Uchikawa et al., 2015) and aragonite (Mavromatis et al., 2015).
392 However, in contrast to the positive relationships between B/Ca and precipitation rate
393 observed previously, we found a negative, albeit weak, correlation between B/Ca and
394 precipitation rate (see supplemental .xls file for rates) or saturation state.

Several possibilities exist to explain the different signs of the effect of precipitation rate on B/Ca between our experiments and previous studies. For studies on calcite, such differences may reflect fundamental differences in how B is incorporated in calcite versus aragonite (e.g. Kitano et al., 1978; Mavromatis et al., 2015), but such an explanation cannot account for differences between our results and those of Mavromatis et al. (2015) for aragonite. However, for experiments conducted at similar [B] to ours, B/Ca data of Mavromatis et al., (2015) correlated with $[B(OH)_4^-]/[CO_3^{2-}]^{0.5}$ (calculated from Table 1 of Mavromatis et al., (2015)) and when expressed as B/Ca / $[B(OH)_4^-]/[CO_3^{2-}]^{0.5}$ their $K_D$ values were consistently lower than those reported here (Table 2). The experiments of Mavromatis et al. (2015) were conducted at lower saturation states than those used in our study; thus such differences may reflect an effect of growth rate on B/Ca which is particularly pronounced at low super-saturation states. It should also be noted that the experiments of Mavromatis et al. (2015) were not conducted using seawater, so the ionic composition of the fluid may influence partitioning (e.g. Kitano et al., 1978).

Alternatively, the expression used for the partition coefficient may play some role in the observed correlations between B/Ca and precipitation rate. Since $K_D$ could be fit almost equally well using saturation state (eq. 6) or $[CO_3^{2-}]$ (eq. 7), any dependence of $K_D$ on $\Omega$ may reflect the dependency of $\Omega$ on $[CO_3^{2-}]$. Thus the dependence of $K_D$ on $[CO_3^{2-}]$ may not reflect a growth rate effect associated with $\Omega$, instead it could indicate that equation 2 does not fully describe the exchange reaction and that the relationship between $B(OH)_4^-$ and $[CO_3^{2-}]$ deviates from the 1 : 0.5 ratio used. Although a few of our experiments were conducted at different $[CO_3^{2-}]$ but similar $\Omega$, and vice-versa, and thus could potentially be

418 used to determine whether [$CO_3^{2-}$] or Ω drives partitioning, no clear pattern was
419 observed.
420 Any influence of temperature or various additives was small relative to other sources of
421 variability as no significant effects were detected, which contrasts with some studies of
422 natural samples as well as one study of synthetic aragonite which point to a temperature
423 effect (Sinclair et al., 1998; Wara et al., 2003; Yu et al., 2007; Mavromatis et al., 2015).
424 It should be noted that because temperature influences saturation state, B and DIC
425 speciation, such effects, if not corrected for, could give rise to an apparent temperature
426 dependency for B/Ca. In the case of Mavromatis et al., (2015), the $K_D$ expression used
427 was based on [B] and not [$B(OH)_4^-$], thus changes in boron speciation with temperature
428 could account for the temperature influence; recalculating their data per equation 2
429 however shows no evidence for a temperature effect on $K_D$ based on the same data
430 points.
431
432 *4.2. Prior $K_D$ estimates*
433 Although the partitioning of B into aragonite has previously been investigated (Kitano et
434 al., 1978; Hemming et al., 1995; Mavromatis et al., 2015), only the study of Mavromatis
435 et al. (2015) characterized carbonate chemistry, thus making it difficult to compare our
436 results with much of the prior work. The experiments of Kitano et al. (1978) were similar
437 to our degassing experiments, but carbonate chemistry was not reported during
438 precipitation; given the range of carbonate chemistry values which can potentially be
439 generated during such an experiment we cannot satisfactorily estimate carbonate
440 chemistry for these experiments. Hemming and Hanson (1992) estimated $K_D$ ~0.012 via

441 equation 1 (or 12 to be consistent with expressing B/Ca as mmol/mol as used elsewhere
442 in our paper) for biogenic calcium carbonate samples, which is well within the range
443 estimated in our study (Table 2). For the experiments of Hemming et al. (1995) detailed
444 carbonate chemistry measurements are lacking, however using their measured pH and
445 calculated [$Ca^{2+}$], and our observation that precipitation typically starts near $\Omega = 20$, we
446 can make rough estimates of the relevant parameters: [$HCO_3^-$] = 1000 µmol/kg, [$CO_3^{2-}$] =
447 100 µmol/kg, and, depending upon the experiment, [$B(OH)_4^-$] = 0.012, 0.107, or 0.78
448 mmol/kg. Using these values, we can estimate $K_D$ via equation 1 and 2 (Table 2).
449 Despite experimental differences, the $K_D$ estimates based on Hemming et al. (1995) fall
450 within the range of values found in the current study. Further, if we use equation 6 to
451 estimate $K_D$ using the above constraints, we would predict a $K_D$ range of 0.08 to 0.04,
452 and with equation 7: 0.09 to 0.05. At the boron concentration closest to seawater used by
453 Hemming et al. (1995), the difference between $K_D$ predicted minus that calculated is -
454 0.001 for equation 6, and 0.01 for equation 7. The range of boron concentrations used by
455 Hemming et al. (1995) includes concentrations well below (~13% of seawater values)
456 those used in the current study, and at [B] well below seawater values, both equations 6
457 and 7 underestimate $K_D$. The study of Mavromatis et al. (2015) included boron
458 concentrations ranging from near seawater values to ~20x seawater values. At high [B],
459 both equation 6 and 7 predict negative $K_D$ values for the Mavromatis et al. (2015) data,
460 indicating that neither equation can be reliably extrapolated far beyond the concentration
461 range used for fitting the equations. Within the range for which [B] was similar,
462 equations 6 and 7 both predicted $K_D$ values higher (up to a factor of 10x) than those
463 calculated from Mavromatis et al. (2015). The highest $\Omega$ (5.8) used by Mavromatis et al.

(2015) was below the lowest values used in the current study, so a growth rate or saturation state influence on $K_D$ could be involved. Our experiment 1c, which precipitated at a lower Ω than any of our other experiments had the lowest $K_D$, consistent with a positive effect of growth rate at low Ω values.

The agreement between $K_D$ estimates both across the diverse conditions used in the current study and for independent studies, suggests that equations 6 and 7 provide reasonable estimates of $K_D$ over a wide range of conditions, except at [B]<<seawater, [B]>>seawater, and Ω<~9.

Table 2. $K_D$ values calculated using different equations for the current study and the studies of Hemming et al. (1995) and Mavromatis et al. (2015). See discussion for further details on the calculations. Note that $K_D$ values expressed here are for expressing B/Ca as mmol/mol. For the current study, mean values are expressed ± 1 standard deviation.

| Study | equation 1 $K_D$ | equation 2 $K_D$ |
|---|---|---|
| Hemming | 4.5 (37 ppm B) -10 (0.59 ppm B) | 0.04 (37 ppm B) - 0.1 (0.59 ppm B) |
| Mavromatis | 0.3 – 40 | 0.0003 – 0.03 |
| Current | 1.4 – 52, mean 23 ± 14 | 0.042 - 0.103, mean 0.071 ± 0.011 |

*4.3. Nernst partition coefficient*

An alternative means of expressing partitioning is to use the single element or Nernst partition coefficient ($D_B$), which is expressed as the ratio of the mass percent B in the solid relative to the mass percent in solution (e.g. Gaetani and Cohen 2006). The use of Nernst partition coefficients allows different studies to be compared as prior studies have generally provided the necessary data. Values for Nernst partition coefficients are dependent upon the specific experimental conditions (temperature, pH, competing species, etc) (e.g. McIntire 1963), as they do not necessarily take into account speciation changes or other factors influencing incorporation, thus comparisons should be interpreted with this in mind. Values for $D_B$ were calculated for each experiment as described for $K_D$ calculations, and are summarized in Table 3 along with those of other studies. $D_B$ values from the current study were strongly correlated with $pH_T$ (pearson correlation coefficient: 0.888), as well as with a wide range of other solution chemistry

parameters (Figure 4), likely reflecting changes in boron and carbon speciation with pH. The following equations described much of the variance in $D_B$ values:

$$D_B = 8.215\ (\pm 0.40)\ pH_T - 0.297\ (\pm 0.035)\ \Omega - 55.69\ (\pm 2.81) \quad \text{eq. 8}$$

$$D_B = 7.954\ (\pm 0.378)\ pH_T - 0.267\ (\pm 0.034)\ \Omega + 0.124\ (\pm 0.038)\ T - 57.3\ (\pm 2.6) \quad \text{eq. 9}$$

$$D_B = 7.429\ (\pm 0.423)\ pH_T - 0.260\ (\pm 0.033)\ \Omega + 0.114\ (\pm 0.037)\ T - 0.491\ (\pm 0.203)\ [B] - 52.5\ (\pm 3.2) \quad \text{eq.10}$$

Where $\Omega$ is the saturation state with respect to aragonite, $pH_T$ is the pH on the total scale, T is temperature in Celsius. All parameter estimates were significant at the $p<0.05$ level, those for the constant, pH and saturation state were all highly significant ($p<0.001$), $R^2$ = 0.9, 0.92, and 0.93 for equation 8, 9, and 10 respectively. Note that $D_B$ depends on factors such as pH and temperature, whereas the $K_D$ values did not, likely reflecting changes in speciation of B and DIC as a function of pH and temperature which were taken into account when calculating $K_D$.

Differences between the predicted (using equation 10) and measured solid composition were not strongly correlated with any solution chemistry parameter, though there was a weak positive correlation with growth rate and with salinity; no significant effects of organic buffers were detected. Relative differences between measured and predicted values were generally less than 16%.

514

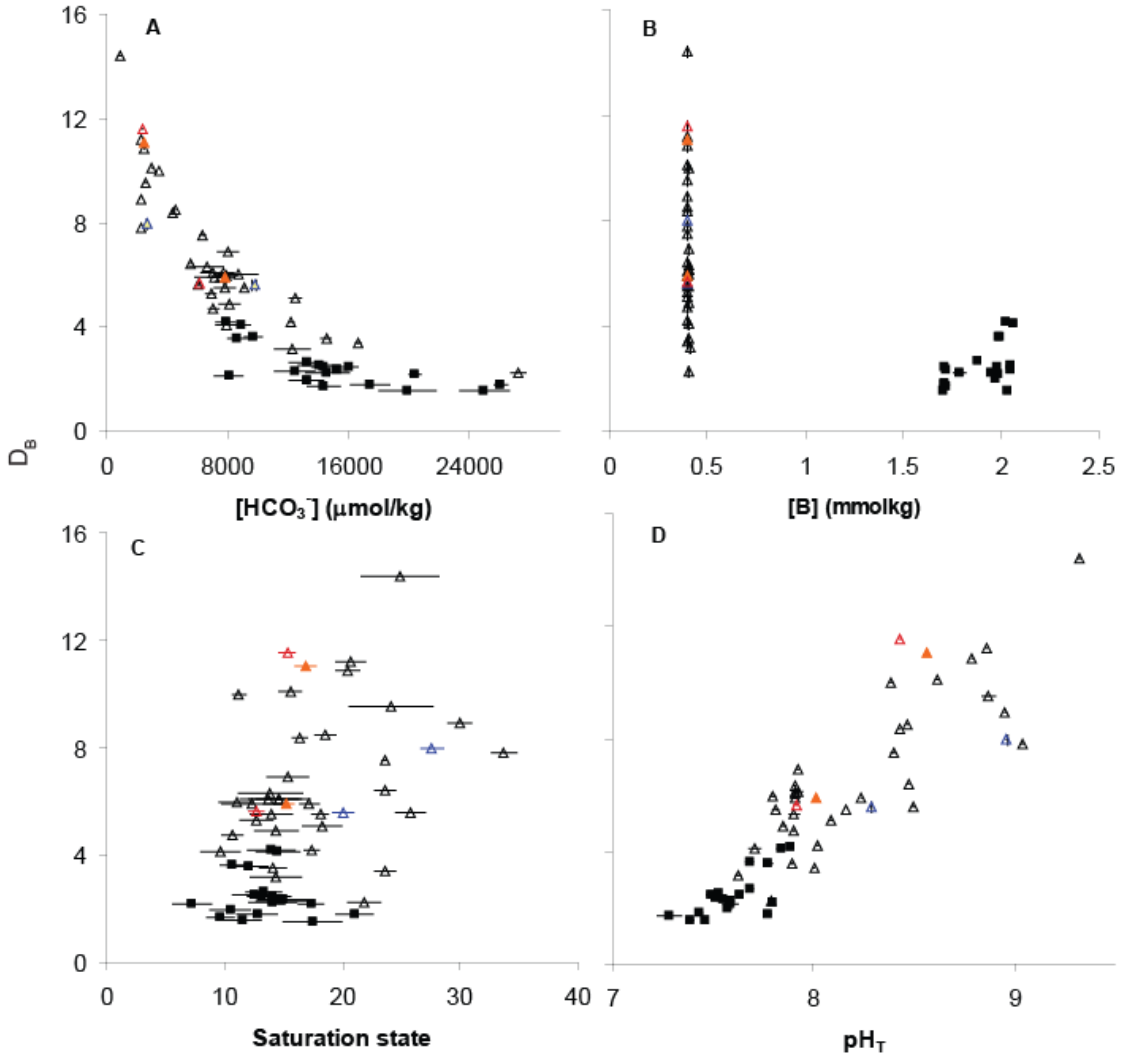


515

516 Figure 4. Relationship between the Nernst partition coefficient ($D_B$) and various solution

517 chemistry parameters. Symbols are as described for figure 2.

518

519 Table 3. Nernst coefficients ($D_B$) estimated from different studies. Note that for

520 estimating $D_B$ for the Hemming and Hanson (1992) study, it was assumed that the

521 biogenic $CaCO_3$ samples precipitated from a solution with 4.676 ppm B, all other studies

522 represent synthetic aragonites and [B] was specified in the study.

| Study | $D_B$ |
|---|---|
| Kitano et al., 1978 | ~0.53 – 1.5 |
| Hemming and Hanson, 1992 | 2-15 |
| Hemming et al., 1995 | 10.2 – 22.8 |
| Mavromatis et al., 2015 | 0.07 – 9 |
| Current | 1.5 – 14.4, mean 5.4 ± 3.0 |

523

524 Our estimates of $D_B$ agree well with existing values – our experimental range covers the
525 range estimated for natural aragonite (Table 3). Our highest values overlap the lower
526 estimates of Hemming et al. (1995); for the two highest [B] used by Hemming et al., their
527 values are only slightly higher than some of our estimates at similar [B]. Estimates of $D_B$
528 from Kitano et al. (1978) and Mavromatis et al. (2015), though below those of Hemming
529 et al. (1995), also overlap our values, with their estimates for their lowest [B] being
530 similar to our values at similar [B]. Although both the $D_B$ values of Kitano et al. (1978)
531 and Hemming et al. (1995) overlap ours, the values in the two studies do not overlap
532 (Table 3). This lack of agreement between these two previous studies likely reflects
533 differences in the carbonate chemistry during aragonite precipitation. In the experiments
534 performed by Hemming et al (1995), $CO_2$ diffusion into the solution controlled
535 precipitation, thus aragonite was formed under low [DIC] and low $[CO_3^{2-}]$ conditions,
536 with $[CO_3^{2-}]$ likely lower than any of our experiments or those of Kitano et al. (1978).
537 Such low $[CO_3^{2-}]$ conditions would in-turn lead to an increase in the $[B(OH)_4^-]/[CO_3^{2-}]^{0.5}$
538 ratio relative to other studies, thus a higher percentage of solution B would be expected to
539 be incorporated into the aragonite, consistent with high $D_B$ estimates (Table 3). In
540 contrast, Kitano et al. (1978) used $CO_2$ degassing experiments, with much lower $[Ca^{2+}]$
541 and higher [DIC]. Although insufficient detail is given to estimate $[CO_3^{2-}]$ for these
542 experiments, concentrations were likely much higher than those of Hemming et al.
543 (1995), potentially similar to ours, consistent with similar $D_B$ estimates. However,
544 Kitano et al. (1978) also used boron concentrations much higher than those used in the
545 current study, and high [B] resulted in lower $D_B$ values.
546 The pattern of lower $D_B$ or $K_D$ values at higher [B] is consistent across studies.

547 Such observations have previously been suggested to be due to saturating defect sites at
548 which incorporation is more favorable at relatively low concentrations leaving only
549 structural sites for further substitution (Hemming et al., 1995). Changes in boron
550 speciation may also occur at high concentrations (e.g. Williams and Strack 1966) which
551 could further affect partitioning. It should also be noted that boron can influence the
552 growth of crystals along different axes (Ruiz-Agudo et al., 2012) and solution chemistry
553 influences surface charging which may further influence B incorporation (Hobbs and
554 Reardon 1999). Although our data provide insight into the controls on B incorporation
555 into aragonite in terms of bulk solution influences, there remains considerable research to
556 be done to understand the detailed mechanisms of B incorporation, particularly with
557 regards to the reactions and molecular rearrangements occurring near the crystal surface,
558 which ultimately control B incorporation and B/Ca ratios.
559
560 *4.4. Environmental proxies*
561 Although our results show patterns consistent with some studies of biologically formed
562 calcium carbonates e.g. $[B(OH)_4^-]/\Delta CO_3^{2-}$ was strongly correlated with B/Ca (Table 1;
563 Yu and Elderfield, 2007), such results cannot be directly compared. Here we directly
564 measure the chemistry during precipitation and thus correlate B/Ca in aragonite to the
565 chemistry in the solution from which that aragonite formed, whereas studies of material
566 in the natural environment usually measure seawater chemistry, not the chemistry of the
567 solution from which precipitation occurs, and thus make an assumption about the link
568 between seawater chemistry and the chemistry of the fluid responsible for precipitation.
569 Biologically formed aragonite is often formed from a solution substantially modified

570 from seawater, for instance, in corals aragonite growth occurs from a solution in which
571 pH and [$CO_3^{2-}$] are elevated relative to the surrounding seawater (e.g. Al-Horani et al.,
572 2003; McCulloch et al., 2012; DeCarlo et al., 2015; Cai et al., 2016). Similarities in
573 relationships between B/Ca and seawater chemistry reported for biological samples and
574 relationships between B/Ca and directly measured solution chemistry in synthetic
575 precipitates suggests that variations in seawater chemistry affect the internal calcifying
576 environment of calcifying organisms. With the relationships described here for synthetic
577 aragonite, B/Ca holds potential as a proxy to determine how the chemistry of the internal
578 calcifying environment of biomineralizing organisms is linked to the external
579 environment. With this framework, B/Ca ratios of the shells and skeletons of calcifying
580 organisms can improve our understanding of how environmental conditions are recorded
581 in biogenic aragonite.
582
583
584 ***5. Summary***
585 The B/Ca ratio in aragonite appears to be primarily a function of $[B(OH)_4^-]/[CO_3^{2-}]^{0.5}$ in
586 the solution from which aragonite growth occurs, with possible influences of [B] and
587 saturation state/[$CO_3^{2-}$]. For aragonites formed from seawater-like solutions, [B] can be
588 estimated from salinity, and since pH can be estimated from boron isotopes (e.g. Trotter
589 et al., 2011), [$B(OH)_4^-$] can be calculated (assuming T is known), thus the remaining
590 variables influencing B/Ca are [$CO_3^{2-}$] and potentially [$Ca^{2+}$]. B/Ca can be used to
591 estimate [$CO_3^{2-}$], thus allowing the full carbonate chemistry under which the aragonite
592 formed to be estimated. If it can be shown that the solution chemistry from which

aragonite precipitates in a particular organism varies in a predictable way with seawater chemistry, it may further be possible to use B/Ca in biogenic carbonates to infer past seawater conditions.

## Acknowledgments

We wish to thank the following for invaluable assistance with this study: R. Belastock, E. Bonk, A. Cohen, D. McCorkle, M. Sulanowska, D. Wellwood, and S. White at Woods Hole Oceanographic Institution; J.P. D'Olivo Cordero, R. Hart, H. Oskierski, K. Rankenburg, K. Tanaka, and J. Trotter at the University of Western Australia. This work was supported by the Australian Research Council (ARC) Centre of Excellence for Coral Reef Studies. Research conducted at WHOI was supported by NSF grant OCE-1338320. M.H. was supported by an ARC Super Science Fellowship and an NSF International Postdoctoral Fellowship. T.D. was supported by a NSF Graduate Research Fellowship. M.M. was supported by a Western Australian Premiers Fellowship and an ARC Laureate Fellowship. The authors acknowledge the facilities, and the scientific and technical assistance of the Australian Microscopy & Microanalysis Research Facility at The University of Western Australia Centre for Microscopy, Characterisation & Analysis, a facility funded by the University, State and Commonwealth Governments.

## References

**Al-Horani FA, Al-Moghrabi SM, de Beer D. 2003.** The mechanism of calcification and its relation to photosynthesis and respiration in the scleractinian coral *Galaxea fascicularis*. Marine Biol **142**: 419-426.

**Allen KA, Hönisch B, Eggins SM, Yu J, Spero HJ, Elderfield H. 2011**. Controls on boron incorporation in cultured tests of the planktic foraminifer *Orbulina universa*. Earth and Planetary Science Letters **309**:291-301 http://dx.doi.org/10.1016/j.epsl.2011.07.010.

**Allen KA, Hönisch B, Eggins SM, Rosenthal Y. 2012.** Environmental controls on B/Ca in calcite tests of the tropical planktic foraminifer species Globigerinoides ruber and

Globigerinoides sacculifer. Earth and Planetary Science Letters **351–352**:270-280 http://dx.doi.org/10.1016/j.epsl.2012.07.004.

**Allison N, Cohen I, Finch AA, Erez J, Tudhope AW. 2014.** Corals concentrate dissolved inorganic carbon to facilitate calcification. Nat Commun **5**10.1038/ncomms6741.

**Babila TL, Rosenthal Y, Conte MH. 2014.** Evaluation of the biogeochemical controls on B/Ca of Globigerinoides ruber white from the Oceanic Flux Program, Bermuda. Earth and Planetary Science Letters **404**:67-76 http://dx.doi.org/10.1016/j.epsl.2014.05.053.

**Burton EA, Walter LM. 1987.** Relative precipitation rates of aragonite and Mg calcite from seawater: Temperature or carbonate ion control? Geology **15**: 111-114

**Cai W-J, Ma Y, Hopkinson BM, Grottoli AG, Warner ME, Ding Q, Hu X, Yuan X, Schoepf V, Xu H, Han C, Melman T, Hoadley KD, Pettay DT, Matsui Y, Baumann JH, Levas S, Ying Y, Wang Y. 2016.** Microelectrode characterization of coral daytime interior pH and carbonate chemistry. Nature Communications **7**:11144

**Culberson C, Pytkowicz RM. 1968.** Effect of pressure on carbonic acid, boric acid, and the pH in seawater. Limnology and Oceanography **13**:403-417

**DeCarlo TM, Gaetani GA, Holcomb M, Cohen AL. 2015.** Experimental determination of factors controlling U/Ca of aragonite precipitated from seawater: Implications for interpreting coral skeleton. Geochimica et Cosmochimica Acta **162**:151-165 http://dx.doi.org/10.1016/j.gca.2015.04.016.

**de Nooijer LJ, Spero HJ, Erez J, Bijma J, Reichart GJ. 2014.** Biomineralization in perforate foraminifera. Earth-Science Reviews **135**:48-58 http://dx.doi.org/10.1016/j.earscirev.2014.03.013.

**Dickson AG. 1990.** Thermodynamics of the dissociation of boric acid in synthetic seawater from 273.15 to 318.15 K. Deep-Sea Research **37**:755-766

**Dissard D, G. Nehrke, G. J. Reichart, J. Nouet, and J. Bijma. 2009.** Effect of the fluorescent indicator calcein on Mg and Sr incorporation into foraminiferal calcite. Geochem Geophys Geosyst **10**:Q11001 doi:10.1029/2009GC002417.

**Douville E, Paterne M, Cabioch G, Louvat P, Gaillardet J, Juillet-Leclerc A, Ayliffe L. 2010.** Abrupt sea surface pH change at the end of the Younger Dryas in the central sub-equatorial Pacific inferred from boron isotope abundance in corals (Porites). Biogeosciences **7**:2445-2459 10.5194/bg-7-2445-2010.

**Foster GL. 2008.** Seawater pH, pCO2 and [CO2−3] variations in the Caribbean Sea over the last 130 kyr: A boron isotope and B/Ca study of planktic foraminifera. Earth and Planetary Science Letters **271**:254-266 10.1016/j.epsl.2008.04.015.

**Gabitov RI, Schmitt AK, Rosner M, McKeegan KD, Gaetani GA, Cohen AL, Watson EB, Harrison TM. 2011.** In situδ7Li, Li/Ca, and Mg/Ca analyses of synthetic aragonites. Geochemistry Geophysics Geosystems **12**10.1029/2010gc003322.

**Gabitov RI, Rollion-Bard C, Tripati A, Sadekov A. 2014.** In situ study of boron partitioning between calcite and fluid at different crystal growth rates. Geochimica et Cosmochimica Acta **137**:81-92 10.1016/j.gca.2014.04.014.

**Gaetani GA, Cohen AL. 2006.** Element partitioning during precipitation of aragonite from seawater: a framework for understanding paleoproxies. Geochimica et Cosmochimica Acta **70**:4617-4634

**Hain MP, Sigman DM, Higgins JA, Haug GH. 2015.** The effects of secular calcium and magnesium concentration changes on the thermodynamics of seawater acid/base chemistry: Implications for Eocene and Cretaceous ocean carbon chemistry and buffering. Global Biogeochemical Cycles **29**:2014GB004986 10.1002/2014gb004986.

**Hathorne EC, Gagnon A, Felis T, Adkins J, Asami R, Boer W, Caillon N, Case D, Cobb KM, Douville E, deMenocal P, Eisenhauer A, Garbe-Schönberg CD, Geibert W, Goldstein S, Hughen K, Inoue M, Kawahata H, Kölling M, Le Cornec F, Linsley BK, McGregor HV, Montagna P, Nurhati IS, Quinn TM, Raddatz J, Rebaubier H, Robinson L, Sadekov A, Sherrell R, Sinclair D, Tudhope AW, Wei G, Wong H, Wu HC, You C-F. 2013.** Inter-laboratory study for coral Sr/Ca and other element/Ca ratio measurements.Geochemistry, Geophysics, Geosystems:n/a-n/a 10.1002/ggge.20230.

**He M, Xiao Y, Jin Z, Liu W, Ma Y, Zhang Y, Luo C. 2013.** Quantification of boron incorporation into synthetic calcite under controlled pH and temperature conditions using a differential solubility technique. Chemical Geology **337–338**:67-74 http://dx.doi.org/10.1016/j.chemgeo.2012.11.013.

**Hemming NG, Hanson GN. 1992.** Boron isotopic composition and concentration in modern marine carbonates. Geochimica et Cosmochimica Acta **56**:537-543 http://dx.doi.org/10.1016/0016-7037(92)90151-8.

**Hemming NG, Reeder RJ, Hanson GN. 1995.** Mineral-fluid partitioning and isotopic fractionation of boron in synthetic calcium carbonate. Geochimica et Cosmochimica Acta **59**:371-379 http://dx.doi.org/10.1016/0016-7037(95)00288-B.

**Henehan MJ, Rae JWB, Foster GL, Erez J, Prentice KC, Kucera M, Bostock HC, Martínez-Botí MA, Milton JA, Wilson PA, Marshall BJ, Elliott T. 2013.** Calibration of the boron isotope proxy in the planktonic foraminifera *Globigerinoides ruber* for use in palaeo-$CO_2$ reconstruction. Earth and Planetary Science Letters **364**:111-122 10.1016/j.epsl.2012.12.029.

**Henehan MJ, Foster GL, Rae JWB, Prentice KC, Erez J, Bostock HC, Marshall BJ, Wilson PA. 2015.** Evaluating the utility of B/Ca ratios in planktic foraminifera as a proxy for the carbonate system: A case study of Globigerinoides ruber. Geochemistry, Geophysics, Geosystems **16**:1052-1069 10.1002/2014gc005514.

**Hobbs MY, Reardon EJ. 1999.** Effect of pH on boron coprecipitation by calcite: Further evidence for nonequilibrium partitioning of trace elements. Geochimica et Cosmochimica Acta **63**:1013-1021

**Holcomb M, Cohen AL, Gabitov RI, Hutter JL. 2009.** Compositional and morphological features of aragonite precipitated experimentally from seawater and biogenically by corals. Geochimica et Cosmochimica Acta **73**:4166-4179 10.1016/j.gca.2009.04.015.

**Kaczmarek K, Langer G, Nehrke G, Horn I, Misra S, Janse M, Bijma J. 2015.** Boron incorporation in the foraminifer Amphistegina lessonii under a decoupled carbonate chemistry. Biogeosciences **12**:1753-1763 10.5194/bg-12-1753-2015.

**Kinsman DJJ, Holland HD. 1969.** The co-precipitation of cations with CaCO3 - IV. The co-precipitation of Sr2+ with aragonite between 16 and 96 C. Geochimica et Cosmochimica Acta **33**: 1-17

**Kitano Y, Okumura M, Idogaki M. 1978.** Coprecipitation of borate-boron with calcium carbonate. Geochemical Journal **12**:183 - 189

**Klochko K, Cody GD, Tossell JA, Dera P, Kaufman AJ. 2009.** Re-evaluating boron speciation in biogenic calcite and aragonite using 11B MAS NMR. Geochimica et Cosmochimica Acta **73**:1890-1900 10.1016/j.gca.2009.01.002.

**Klochko K, Kaufman AJ, Yao W, Byrne RH, Tossell JA. 2006.** Experimental measurement of boron isotope fractionation in seawater. Earth and Planetary Science Letters **248**:276-285 10.1016/j.epsl.2006.05.034.

**Mass T, Drake JL, Haramaty L, Kim JD, Zelzion E, Bhattacharya D, Falkowski PG. 2013.** Cloning and characterization of four novel coral acid-rich proteins that precipitate carbonates in vitro. Current Biology **23**:1126-1131 10.1016/j.cub.2013.05.007.

**Mavromatis V, Montouillout V, Noireaux J, Gaillardet J, Schott J. 2015**. Characterization of boron incorporation and speciation in calcite and aragonite from co-precipitation experiments under controlled pH, temperature and precipitation rate. Geochimica et Cosmochimica Acta 150: 299-313

**McCulloch M, Falter J, Trotter J, Montagna P. 2012.** Coral resilience to ocean acidification and global warming through pH up-regulation. Nature Clim Change **2**:623-627

**McIntire WL. 1963.** Trace element partition coefficients - a review of theory and applications to geology. Geochimica et Cosmochimica Acta **27**:1209-1264

**Ni Y, Foster GL, Bailey T, Elliott T, Schmidt DN, Pearson P, Haley B, Coath C. 2007.** A core top assessment of proxies for the ocean carbonate system in surface-dwelling foraminifers. Paleoceanography **22**:n/a-n/a 10.1029/2006pa001337.

**Pearson PN, Palmer MR. 1999.** Middle Eocene Seawater pH and Atmospheric Carbon Dioxide Concentrations. Science **284**:1824-1826 10.1126/science.284.5421.1824.

729 **Pelejero C, Calvo E, McCulloch MT, Marshall JF, Gagan MK, Lough JM, Opdyke BN. 2005.**
730 Preindustrial to Modern Interdecadal Variability in Coral Reef pH. Science **309**:2204-2207
731 **Penman DE, Hönisch B, Rasbury ET, Hemming NG, Spero HJ. 2013.** Boron, carbon, and
732 oxygen isotopic composition of brachiopod shells: Intra-shell variability, controls, and potential
733 as a paleo-pH recorder. Chemical Geology **340**:32-39 10.1016/j.chemgeo.2012.11.016.
734 **Rae JWB, Foster GL, Schmidt DN, Elliott T. 2011.** Boron isotopes and B/Ca in benthic
735 foraminifera: Proxies for the deep ocean carbonate system. Earth and Planetary Science
736 Letters **302**:403-413 10.1016/j.epsl.2010.12.034.
737 **Rollion-Bard C, Blamart D, Trebosc J, Tricot G, Mussi A, Cuif J-P. 2011.** Boron isotopes as
738 pH proxy: A new look at boron speciation in deep-sea corals using 11B MAS NMR and EELS.
739 Geochimica et Cosmochimica Acta **75**:1003-1012 10.1016/j.gca.2010.11.023.
740 **Ruiz-Agudo E, Putnis CV, Kowacz M, Ortega-Huertas M, Putnis A. 2012.** Boron incorporation
741 into calcite during growth: Implications for the use of boron in carbonates as a pH proxy. Earth
742 and Planetary Science Letters **345-348**:9-17 10.1016/j.epsl.2012.06.032.
743 **Sanyal A, Hemming NG, Broecker WS, Lea DW, Spero HJ, Hanson GN. 1996.** Oceanic pH
744 control on the boron isotopic composition of foraminifera: Evidence from culture experiments.
745 Paleoceanography **11**:513-517 10.1029/96pa01858.
746 **Sanyal A, Nugent M, Reeder RJ, Bigma J. 2000.** Seawater pH control on the boron isotopic
747 composition of calcite: evidence from inorganic calcite precipitation experiments. Geochimica et
748 Cosmochimica Acta **64**: 1551-1555
749 **Sen S, Stebbins JF, Hemming NG, Ghosh B. 1994.** Coordination environments of B impurities
750 in calcite and aragonite polymorphs: A 11B MAS NMR study. American Mineralogist **79**:819-
751 825
752 **Sinclair DJ, Kinsley LPJ, McCulloch MT. 1998.** High resolution analysis of trace elements in
753 corals by laser ablation ICP-MS. Geochimica et Cosmochimica Acta **62**: 1889-1901
754 **Tripati AK, Roberts CD, Eagle RA, Li G. 2011.** A 20 million year record of planktic foraminiferal
755 B/Ca ratios: Systematics and uncertainties in pCO2 reconstructions. Geochimica et
756 Cosmochimica Acta **75**:2582-2610 http://dx.doi.org/10.1016/j.gca.2011.01.018.

**Trotter J, Montagna P, McCulloch M, Silenzi S, Reynaud S, Mortimer G, Martin S, Ferrier-Pagès C, Gattuso J-P, Rodolfo-Metalpa R. 2011.** Quantifying the pH 'vital effect' in the temperate zooxanthellate coral Cladocora caespitosa: Validation of the boron seawater pH proxy. Earth and Planetary Science Letters **303**:163-173 10.1016/j.epsl.2011.01.030.

**Uchikawa J, Penman DE, Zachos JC, Zeebe RE. 2015.** Experimental evidence for kinetic effects on B/Ca in synthetic calcite: Implications for potential B(OH)4− and B(OH)3 incorporation. Geochimica et Cosmochimica Acta **150**:171-191 10.1016/j.gca.2014.11.022.

**van Heuven S, Pierrot D, Lewis E,Wallace DWR. 2009.** MATLAB Program developed for $CO_2$ system calculations. ORNL/CDIAC-105b. Carbon Dioxide Information Analysis Center, Oak Ridge National Laboratory, U.S. Department of Energy, Oak Ridge, TN.

**Venn AA, Tambutte E, Holcomb M, Laurent J, Allemand D, Tambutte S. 2013.** Impact of seawater acidification on pH at the tissue-skeleton interface and calcification in reef corals. Proc Natl Acad Sci U S A **110**:1634-1639 10.1073/pnas.1216153110.

**Wang Z, Hu P, Gaetani G, Liu C, Saenger C, Cohen A, Hart S. 2013.** Experimental calibration of Mg isotope fractionation between aragonite and seawater. Geochimica et Cosmochimica Acta **102**:113-123 10.1016/j.gca.2012.10.022.

**Wara MW, Delaney ML, Bullen TD, Ravelo AC. 2003.** Possible roles of pH, temperature, and partial dissolution in determining boron concentration and isotopic composition in planktonic foraminifera. Paleoceanography **18**:n/a-n/a 10.1029/2002pa000797.

**Williams PM, Strack PM. 1966.** Complexes of boric acid with organic cis-diols in seawater. Limnology and Oceanography **11**:401-404

**Wolthers M, Nehrke G, Gustafsson JP, Van Cappellen P. 2012.** Calcite growth kinetics: Modeling the effect of solution stoichiometry. Geochimica et Cosmochimica Acta **77**:121-134 http://dx.doi.org/10.1016/j.gca.2011.11.003.

**Xiao Y, Li H, Liu W, Wang X, Jiang S. 2008.** Boron isotopic fractionation in laboratory inorganic carbonate precipitation: evidence for the incorporation of B(OH)3 into carbonate. Science in China Series D: Earth Sciences **51**:1776-1785 10.1007/s11430-008-0144-y.

784 **Yu J, Elderfield H. 2007.** Benthic foraminiferal B/Ca ratios reflect deep water carbonate
785 saturation state. Earth and Planetary Science Letters **258**:73-86 10.1016/j.epsl.2007.03.025.
786 **Yu J, Elderfield H, Hönisch B. 2007.** B/Ca in planktonic foraminifera as a proxy for surface
787 seawater pH. Paleoceanography **22**:n/a-n/a 10.1029/2006pa001347.
788
789
790

**Supplemental materials**

Detailed methods and associated discussion, figures, and tables

*S1. Precipitation details*

*S1.1. Reagents*

Seawater drawn continuously from ~4 m depth, ~200 m off-shore in Vineyard Sound (Massachusetts, USA), passed through a sand filter and distributed throughout the Environmental Systems Laboratory (WHOI) was used for all experiments. The seawater used for experiments was further passed through pleated Flow Max cartridge filters (final size 0.35 μm), and finally a 0.2 μm Whatman Polycap 36tc filter (lot y830) and stored in HDPE carboys (all filters and carboys were rinsed repeatedly prior to collecting seawater). Seawater was collected on three different dates in 2011 and 2013 and stored in the dark for no more than 6 weeks prior to use in experiments.

Concentrated seawater (2xsw) was prepared by placing seawater in pre-washed ~1 L polypropylene (PP) containers (MicroLite, Anchor Packaging) held within warm water baths (50 – 70 $^{o}$C) and allowing it to evaporate until the mass halved. 2xsw used in 2011 was not filtered, while that used in 2013 was passed through a 0.45 μm filter (Millipore HAWP) prior to use.

Calcium carbonate was from Alfa Aesar (puratronic stock 43073 lot l16Q78 - used for runs in 2011 and degassing runs 1-4 in 2013, or stock 10996 lot C24U037 for runs 5 - 7 in 2013 as well as the fsw containing $CaCO_3$ used in pumping runs 13g and 8f).

Strontium carbonate was from Alfa Aesar (puratronic stock 36618, lot 23557 used in 2011, lot 23399 in 2013), as was sodium carbonate (puratronic stock 10861 lot 23390 or

814 23776). Other reagents were obtained from various suppliers: $NaHCO_3$ (Acros
815 424270010 lot a0200805001 for 2011 and 13g, 10h, 6c, and 7d in 2013; Alfa Aesar stock
816 10863 lot S70421 for other 2013 experiments), calcein (Alfa Aesar L10255 lot
817 10132899), OTC (oxytetracycline dihydrate, Acros 123840100 lot A0275864), TRIS
818 base (Fisher t395 lot 064221 used in 2011, or lot 104689 used in 2013), $Na_2B_4O_7$ $10H_2O$
819 (Baker 3568 lot C13634), NaOH (Fisher s318 lot 975017), HEPES sodium salt (Fisher
820 BP2939 lot 107739), $CaCl_2$ (Alfa Aesar 10043-52-4, stock L13191 lot 10113722), $MgCl_2$
821 (Alfa Aesar stock 12315 lot f18w011).
822 Water used for preparing solutions and cleaning was either quartz distilled (used in 2011)
823 or filtered (18 MΩ, Barnstead Nanopure; used in 2013).
824
825 *S.1.2. Aragonite growth set-up*
826 All experiments conducted in 2011 used ~1 L PET containers (Deli Gourmet, Solo) for
827 aragonite growth, while in 2013 ~1 L PP containers (MicroLite, Anchor Packaging) were
828 used for most experiments. The choice of container has little impact on the experiment
829 (unpublished data). Precipitates grown in PET containers were generally easier to
830 recover than those grown in PP containers, but, PET tends to be damaged by acid
831 washing, thus when precipitates were to be used primarily for trace element composition
832 and thus all glass and plastic ware acid (HCl) washed prior to use, PP containers were
833 used.
834
835 Some experiments were bubbled with air, $CO_2$, or mixtures there-of. Air/$CO_2$ mixtures
836 were prepared using mass flow controllers. The $pCO_2$ of both the mixed gasses and air

837 was determined using a NDIR $CO_2$ analyzer (Qubit S-151). Atmospheric pressure in the
838 lab was recorded (dial barometer, Fisher) each time the gas composition was measured –
839 values were generally near 770 mmHg. Gas flows to individual experiments were
840 controlled with rotameters. All gasses were bubbled through de-ionized water prior to
841 being introduced into experimental containers to humidify the air and thus reduce
842 evaporation of the experimental solution. Gasses were introduced into a given
843 experiment via a glass tube with a glass frit to diffuse the air near the bottom of each
844 experimental container.
845
846 For pumping experiments, glass and teflon syringes (SGE gastight) were used to add
847 reagents in 2011, polypropylene/polyethylene syringes (Norm-ject, Henke-Sass Wolf) in
848 2013. Vinyl tubing (Cole-Parmer 30526-18) was used to carry reagents from the syringe
849 to the experimental container. Syringes and tubing were washed with dilute HCl, $H_2O$,
850 and the given reagent prior to use.
851 Details specific to individual experiments are provided in Table S1.
852
853 *S1.3. Weights*
854 All solutions added to or removed from an experiment were weighed using an Ohaus
855 precision standard model ts4kd balance, the calibration was verified using reference
856 masses prior to each group of experiments (measured reference values were within 0.03%
857 of expected). Most reagents and all dilutions of alkalinity samples were weighed to four
858 or five decimal places (Sartorius cpa124s or bp211d balances); reference weights were
859 within 0.006% of expected values.

860

861 *S1.4. Stirring*

862 All solutions were stirred continuously during precipitation. This was affected using one
863 of three different methods. An overhead stirrer set at 120 rpm was used to rotate a PTFE
864 impeller with 4 angled blades (~4 cm diameter) for all 2013 experiments ending "g" or
865 "h" and 2011 experiments ending "1" or "2". Experiments ending a-f were stirred with
866 PTFE coated octagonal magnetic stir bars ~5.1 cm long and 0.8 cm diameter at a rate of
867 130 rpm. In 2011, stir bars were placed directly on the bottom of the containers. To
868 reduce problems with the stir bar grinding the growing precipitates, stir bars were
869 suspended ~2 cm from the bottom of the container using nylon monofilament line for
870 experiments conducted in 2013. The line was attached to a swivel, thus the stir bar could
871 rotate freely.

872

873 *S2. Solution chemistry and calculations*

874 *S2.1. Salinity*

875 The final salinity as well as the initial salinity of seawater based reagents was
876 measured using a conductivity probe (Hach). Conductivity values were converted to
877 salinity using equations of Fofonoff (1985). The initial seawater and a sub-set of final
878 solutions were also measured using a Guildline autosal model 8400B salinometer.
879 IAPSO standard seawater (batch P-153) was used to standardize the autosal before runs.
880 For samples measured using both methods, agreement was generally within 0.5, though
881 values measured using the Hach conductivity probe were invariably offset from the

882 autosal values, thus a correction was applied to the values measured using the Hach probe
883 to better match the autosal values.
884
885 *S2.2. Alkalinity and pH*
886 Alkalinity measurements were carried out per Holcomb et al. (2012), most samples were
887 diluted with a ~39 g NaCl/L solution at the time of collection to prevent precipitation
888 prior to measurement and to reduce the alkalinity to <5200 μmol alkalinity/kg sw. When
889 appropriate, the calculations were corrected for the presence of added buffers. Due to the
890 experimental solutions departing from seawater composition, a number of modifications
891 were made to otherwise standard calculations – see section S2.3.
892 All pH measurements (recorded to 0.1 mV) were made on unfiltered samples using an
893 Orion Ross 8165 pH electrode and an Orion 3-star meter calibrated against NBS buffers
894 (Ricca). Solutions for pH measurement were placed in a tube in a temperature controlled
895 bath (~ 25 $^{o}$C) and stirred during pH measurement. Periodic measurements of either
896 certified seawater reference material (CRM-107 or 117, supplied by Andrew Dickson,
897 Scripps Institute of Oceanography) or an in-house standard were made to estimate the
898 offset between $pH_{NBS}$ and $pH_T$. The $pH_T$ for the standard seawater solutions was
899 calculated based on TA and DIC using CO2Sys (van Heuven et al., 2009) with constants
900 from Mehrbach et al. (1973) as refit by Dickson and Millero (1987), and Dickson (1990)
901 for sulfate. Measurements were then corrected to the total scale assuming that drift in the
902 offset value was linear with time between times at which it was determined.
903 Occasionally values for alkalinity or pH were not obtained at a given measurement time-
904 point. When this occurred, values were interpolated based on measurements made before

905 and after the missing value and calculated rates of alkalinity depletion – the rate of
906 alkalinity depletion was assumed to remain stable over the period affected by a missing
907 alkalinity value.
908
909
910 *S2.3. Salinity corrections*
911 Due to the addition of different compounds to seawater, standard seawater salinity to
912 composition and ion activity relationships do not apply to most time-points in our
913 experiments. For example, addition of $MgCl_2$ adds conductivity (and thus changes
914 salinity) and affects ion activities, yet makes no contribution to alkalinity, nor does it
915 contribute other species which usually vary in direct proportion to salinity. A number of
916 calculations (titration alkalinity, carbonate chemistry parameters, etc.) make use of
917 salinity to composition relationships to simplify calculations. To compensate for
918 compositional differences, a number of modifications were made to these otherwise
919 standard calculations.
920
921 *S2.3.1. Titration alkalinity corrections*
922 For the calculation of titration alkalinity, a regression analysis was used (Holcomb et al.,
923 2012). This code uses salinity to concentration relationships to calculate concentrations
924 of B, F, etc., as well as salinity dependencies for estimating carbonate equilibrium
925 constants. The concentrations of $NH_4$, $H_2SiO_4$, and $PO_4$ were assumed to be 0 in all
926 solutions, and all reagents used were assumed to be free from compounds that would
927 affect alkalinity calculations except for those specifically considered. TRIS, HEPES, and

928 boron were added to certain experiments. The contribution of boron is normally
929 considered in calculating alkalinity, so only the B concentration was adjusted to account
930 for the added B. To account for the contribution of TRIS we used a pKa value calculated
931 from equation 27 of Dickson (1993). For HEPES, we are unaware of reported pKa
932 values for seawater media, thus a pKa of 7.5 was assumed. Since most alkalinity samples
933 were diluted with a NaCl solution (~39 g NaCl/L – with an assumed salinity of 32 and no
934 contribution to alkalinity), concentrations of different species (B, F, etc.) and salinities
935 were corrected for sample dilution. Due to the addition of various reagents over the
936 course of each experiment, the measured final salinities (calculated from conductivity) do
937 not reflect seawater composition, nor do they capture the evolution of solution chemistry
938 over time. However, for most pumping experiments, the error introduced by ignoring
939 such salinity changes is less than 1 μmol alkalinity/kg sw, whereas the typical relative
940 standard deviation for repeated alkalinity measurements is 0.2%, or ±5 μmol alkalinity/kg
941 sw at a typical seawater alkalinity, thus no attempt was made to further correct salinity,
942 and the final measured salinity was used for calculations. For degassing experiments
943 there was a greater difference between measured salinity and that of seawater (due to the
944 addition of $MgCl_2$), thus a salinity of 32.5 was used for calculating the concentrations of
945 different species in the experimental fluid, while the measured final salinity was used for
946 calculating equilibrium constants. All NaX solutions were assumed to have a salinity of
947 0 for calculating concentrations of species contributing to alkalinity, and S = 4.5 for
948 calculating equilibrium constants – though due to samples being substantially diluted
949 with the NaCl solution prior to measurement, the final salinity used for calculating
950 constants was invariably near 32.

951

952 *S2.3.2. Carbonate chemistry corrections*

953 Calculations of the full carbonate system chemistry and concentrations of different
954 species are more sensitive to errors in salinity estimates than titration alkalinity
955 calculations, thus a more rigorous set of corrections were used for these calculations.
956 Two different salinity values were used for calculations. The empirical equilibrium
957 constants used for calculating inorganic carbon, boron, etc. speciation are functions of
958 salinity (reflecting the influence of ionic strength on ion activities). Thus the addition of
959 ions (such as contributed by NaX solutions, or $MgCl_2$) affects salinity, ionic strength, and
960 in-turn, equilibrium constants. Although the influence of the ions added in this
961 experiment on equilibrium constants likely differs from that expected based purely on
962 changes in salinity (estimated from conductivity), we assumed that the compositional
963 changes were sufficiently small that seawater derived salinity relationships could still be
964 used for calculating equilibrium constants. For estimating concentrations of species such
965 as B, F, $SO_4$, Ca, etc., the measured salinity values could not be used due to ions added
966 with the NaX or $MgCl_2$ solutions contributing to salinity but not affecting concentrations
967 of other species present in seawater. Thus, measured salinities were corrected for the
968 contribution of the added ions. The ionic equivalent conductivities reported by
969 Pawlowicz (2010) were used to estimate the contribution of the added NaX or $MgCl_2$ to
970 conductivity, and equations from Fofonoff (1985) to convert conductivity to salinity.
971 Due to differences in how different experiments were conducted, slightly different
972 procedures were used for calculating salinity at different time-points.

973

For degassing experiments, the initial salinity of the solution was unknown due to evaporation potentially occurring during the dissolution of reagents with $CO_2$. The final measured salinity was however known. Since the degassing experiments used a modified seawater solution in which the primary salt added was $MgCl_2$, the salinity values used for calculating concentrations were corrected for the presence of $MgCl_2$ by subtracting the $MgCl_2$ contribution from the total salinity. To compensate for evaporation, the evaporation rate was estimated from the difference in expected and measured final solution mass relative to the total time for each experiment. For each group of experiments (run simultaneously from the same starting solution), the median evaporation rate was used to correct the salinity for each time point. Most experiments from a given group were run for a similar length of time and had similar evaporation rates (typically 0.5 to 2 g/day, depending upon the set of experiments; excluding suspect values, the range within a group was less than 0.7 g/day), but one experiment departed from this pattern (we suspect the final weight recorded was incorrect). By using the median evaporation rate for each group of experiments we were able to avoid one potentially erroneous value influencing the interpretation. Precipitation of $CaCO_3$ was not included in correcting salinity values as it had relatively little impact.

For pumping experiments, the salinity of the initial seawater was known, thus the expected salinity at any point in time could be calculated based on the initial salinity and the salinity of solutions added to the experiment. The 2xsw solution was assumed to have a salinity of 64, which contributed both to the salinity value used to calculate constants and to that used for concentrations. The sw solution containing $CaCO_3$ and

997 $SrCO_3$ added in two of the pumping experiments was assumed to have S = 31.9. The
998 NaX solutions were assumed to contribute nothing to the salinity value used to calculate
999 concentrations, but for constants, contributed 3, 2.5, 2, and 0.75 to the salinity for
1000 $NaHCO_3$, $NaHCO_3/Na_2CO_3$, $Na_2CO_3$, and $Na_2CO_3$ added during the period in which
1001 precipitation was occurring respectively. The use of 0.75 during precipitation reflects an
1002 assumption that for every unit of $Na_2CO_3$ added, a unit of $CaCO_3$ precipitates, thus
1003 reducing the overall change in salinity. Based on the measured final salinity, an
1004 evaporation rate was calculated to allow the expected salinity to match (within 0.1) the
1005 measured salinity. Using the salinity based evaporation rate the expected final mass was
1006 calculated, values were generally in good agreement with measured values (difference of
1007 1 ± 2 g (average ± standard deviation, excluding one suspect value)).
1008 To calculate carbonate chemistry and borate concentrations, a Matlab version of CO2sys
1009 (adapted from van Heuven et al., 2009, using constants from Mehrbach et al., 1973 as fit
1010 by Dickson and Millero 1987; Dickson 1990 for borate, and Dickson 1990 for sulfate)
1011 was used. In addition to the standard species considered, additional buffers were
1012 included (per alkalinity calculations, see above), and boron concentrations were
1013 calculated based on the boron:salinity relationship of Lee et al. (2010), plus any added
1014 boron when appropriate. Although nutrient chemistry was not measured in the seawater
1015 batches used in these experiments, previous studies have monitored nutrients in seawater
1016 from the same source (Holcomb et al., 2010; 2012), based on these data we assumed $NH_3$
1017 = 0, $H_2SiO_4$ = 5, and $PO_4$ = 0.25 μmol/kg sw at S=32 for all calculations. A wide range
1018 of species ($SO_4^{2-}$, $F^-$, etc.) are incorporated into aragonite and could influence the
1019 calculation of carbonate chemistry, however the likely effects were deemed insufficient

1020 to justify corrections in the calculation of carbonate chemistry (a typical S/Ca ratio
1021 measured in a synthetic precipitate was ~6 mmol/mol (unpublished data), which,
1022 assuming a concentration of 28 mmol $SO_4^{2-}$/kg sw represents less that 0.5% removed by
1023 the precipitate; for F, although a greater percentage of total F was removed (~5
1024 mmol/mol Tanaka et al., unpublished data), the low concentration present in seawater
1025 combined with the low pKa should result in little effect on alkalinity). Although the
1026 amount of boron removed by precipitation was trivial relative to measurement
1027 uncertainty, values were corrected by assuming the precipitate formed with a constant
1028 B/Ca ratio and the amount of precipitate formed corresponded to the difference between
1029 measured and expected (assuming no precipitation) alkalinity. $Ca^{2+}$ values used to
1030 calculate saturation states were corrected for added calcium or calcium removed (based
1031 on the expected calcium concentration and the amount of calcium removed as estimated
1032 from alkalinity depletion). For a subset of experiments, solution [$Ca^{2+}$] was measured
1033 (DeCarlo et al., 2015). Measured values showed similar patterns to calculated values,
1034 though measured values tended to be ~0.5 mmol/kg higher than expected.
1035
1036 *S3. ICPMS measurements*
1037 *S3.1. X-Series*
1038 Preparation of aragonite samples for measurement of B/Ca (and other element) ratios via
1039 Q-ICPMS (X-Series II, Thermo Fisher Scientific) followed standard protocols (Holcomb
1040 et al., 2015). Briefly powders were rinsed repeatedly with $H_2O$ (18.2 MΩ, Millipore
1041 Integral 5), and most were cleaned with NaOCl. Cleaned powders were dried, weighed
1042 (~20 mg sub-sample), and dissolved in ~0.58 N $HNO_3$ (prepared from sub-boiling

1043 distilled (Savillex DST-1000) $HNO_3$), final acid concentration ~0.1 N. For X-Series
1044 measurements, samples were diluted in 2% $HNO_3$ containing various elemental spikes to
1045 a final concentration of ~100 ppm Ca or 10 ppm Ca, depending upon the elements to be
1046 measured (e.g. Zinke et al., 2014; Holcomb et al., 2015). The coral standard JCp-1 was
1047 used as the standard, with an accepted B/Ca ratio of 0.4596 mmol B/mol Ca (Hathorne et
1048 al., 2013).
1049 Ca measurements were also carried out on the X-Series using the same solutions used for
1050 measuring elemental ratios. Standards containing various concentrations of [Ca]
1051 (prepared from a 10000 ppm Ca standard (Fisher j/8240 lot 1147827)) were run to
1052 calibrate Ca count ratios relative to the Sc spike included in all solutions.
1053
1054 *S3.1.1. Sample purity*
1055 Aragonite is known to contain a wide range of cations and anions other than $Ca^{2+}$ and
1056 $CO_3^{2-}$, with concentrations of each approaching 50 mmol/mol in aragonite formed in
1057 marine environments. Thus assuming just $CaCO_3$ is present may bias results. However,
1058 given our measurement reproducibility (~1.5%), fairly large changes in the composition
1059 of the sample would be needed before we would be able to identify a change in Ca. This
1060 is consistent with our measured calcium contents giving an average of 0.010 mol Ca/g
1061 sample, the value expected for pure $CaCO_3$. We thus considered the precipitates to be
1062 composed of pure $CaCO_3$ for calculations, though for illustration purposes we include
1063 one figure with B normalized to the measured Ca content in addition to mass based (Fig.
1064 S1).
1065

*S3.2. MC-ICPMS*

Boron in most samples was measured via MC-ICPMS (Neptune Plus, ThermoFisher Scientific or NU Plasma II, NU instruments). Cation and anion resin purification procedures were used for all aragonite samples (McCulloch et al., 2014), except the solutions were weighed to the nearest 0.00001 g to allow for more accurate calculation of B concentrations. A subset of samples was also prepared with the chemistry described in section S3.3. Boron concentrations were estimated based on the total B 10+11 intensity for the sample relative to bracketing standards of known [B]. B/Ca ratios in aragonite samples were calculated based on both the sample mass and the measured [Ca] (from X-Series measurements).

*S3.2.1. Agreement amongst B/Ca estimates*

The validity of measurements of B/Ca ratios made using the X-Series could be compromised due to the use of the coral standard JCp-1 to calculate all ratios, despite some of the synthetic aragonites having B/Ca ratios substantially different from JCp-1 (ranging from ~0.1 to 0.9 mmol/mol versus a value of 0.4596 mmol/mol for JCp-1). Although all measurements were made at similar Ca concentrations, B concentrations could deviate substantially from those of the standard, thus any non-linearity in the response could bias calculated ratios. To assess any potential bias in the X-Series measurements, B/Ca was also estimated from boron measurements made via MC-ICP-MS. Repeated measurements of B/Ca ratios made on different days via the X-Series gave a reproducibility (1 standard deviation) of 0.02 mmol B/mol Ca or better for any given sample, while MC-ICP-MS based measurements were reproducible to better than

1089 0.04 mmol B/mol Ca (1 standard deviation). In all cases the average standard deviation
1090 was less than 0.01 mmol/mol. Ratios determined with the X-Series differed from those
1091 determined via MC-ICP-MS. However, on average X-Series measurements were 0.016
1092 mmol/mol lower, which is within measurement error. The relationship between
1093 measurements made with the X-Series, and those made via MC-ICP-MS using different
1094 extraction and normalization approaches is shown in Fig. S1.
1095
1096 *S3.3. B purification chemistry using TRIS*
1097 Since seawater samples contain ions not efficiently removed by the cation/anion resins
1098 used for carbonate samples (Holcomb et al., 2014; McCulloch et al., 2014), the boron
1099 specific resin Amberlite IRA 743 was used to purify the B from solution. Although
1100 several protocols exist for purifying boron using this resin (e.g. Lecuyer et al., 2002;
1101 Lemarchand et al., 2002; Foster 2008; Trotter et al., 2011; Dissard et al., 2012), existing
1102 protocols require either careful control of pH during boron absorption to avoid the
1103 formation of precipitates, pre- or post-purification, or are conducted under low pH
1104 conditions at which the capacity of the resin to absorb boron is reduced. To avoid these
1105 problems, we used an organic buffer, TRIS (Tris(hydroxymethyl)aminomethane), to
1106 stabilize the pH during boron absorption at ~8, thus reducing problems with hydroxides
1107 precipitating yet allowing boron absorption to occur at relatively high pH, thus taking
1108 advantage of the absorption capacity of the resin. To a 5 ml polypropylene tube we
1109 added ~0.05 ml of pre-cleaned Amberlite resin (in 0.075 N $HNO_3$), 2.5 ml $H_2O$
1110 containing ~0.01 mg phenol red, varying amounts of sample (typically 0.1 ml, though for
1111 NaX solutions and other samples expected to have low [B] 0.4 ml were used), and TRIS

buffer (0.5:1 to 2:1 ratio TRIS to sample volume, depending upon the nature of the sample). The TRIS buffer solution used was ~ 0.3 M TRIS (Acros 424571000 lot A0326538) prepared in ~ 0.07 N $HNO_3$ and stored in contact with Amberlite IRA 743 resin. TRIS was prepared in dilute acid to limit the possibility of achieving too high a pH. Samples were incubated overnight on a shaker table, the supernatant discarded, resin rinsed 4x with $H_2O$, and then the boron eluted with 4 successive 0.6 ml volumes of 0.15 N $HNO_3$ with at least 6 h incubation on the shaker table for each elution volume. In addition to solution samples, some precipitates and coral standards were also extracted following this protocol – precipitates were dissolved as described above prior to extraction. Nitric acid blanks were extracted as well to verify procedural blanks each time samples were extracted.

*S3.4. Validating TRIS extraction*

To verify the veracity of the TRIS based extraction protocol, a number of samples were prepared using both the method described above as well as established techniques using either cation and anion column chemistry (McCulloch et al., 2014), or traditional amberlite based extraction techniques using NaOH to adjust the pH (e.g. Holcomb et al., 2014). Results show similar B/Ca ratios for aragonite samples prepared with the various methods (Fig. S1). Repeated measurements of seawater samples prepared with amberlite resin and TRIS gave a reproducibility of boron concentration estimates of better than 6% RSD, with an average reproducibility of 1.6% RSD. Measured seawater boron concentrations agreed with calculated concentrations with an average difference of <0.2%.

*S4. XRD and Raman*

Verification of the mineral form present in all experiments run in 2013 was made via powder x-ray diffraction (XRD). Precipitates were loaded onto a Si holder on a rotating stage and diffraction patterns collected using a PANalytical Empyrean diffractometer (at the Centre for Microscopy, Characterisation & Analysis, UWA) using Ni filtered Cu Kα radiation (generator at 40 kV, current 40 mA). For reference purposes, a coral aragonite sample was run each day patterns were obtained for precipitates. A subset of experiments run in 2011 were characterized by XRD at WHOI by M. Sulanowska. A raman microscope was also used to determine the mineralogy of individual grains for many of the experiments per Holcomb et al. (2009) for experiments run in 2011; DeCarlo et al. (2015) for experiments run in 2013.

In one experiment, in which precipitation was induced by adding a solution containing NaOH (experiment 11h) $Mg(OH)_2$ was likely formed, however no clear peaks associated with $Mg(OH)_2$ were detected with Raman nor XRD. Visual observation of the sample suggested aragonite was not the primary phase, and the elemental composition showed Mg/Ca ratios (~ 100x typical aragonite values) inconsistent with aragonite being the only phase present. Such observations point to a need for caution in relying on any single means of identifying the mineral phase formed in synthetic experiments – for instance, although XRD patterns for sample 11h were atypical (weak peak near $2\theta = 19^{o}$), aragonite peaks were clearly present (Fig. S2). Given the wide range of peak shapes/heights observed for different precipitates (likely reflecting variations in crystal sizes and orientations amongst experiments), the presence of a phase other than aragonite

would not necessarily have been detected from an XRD pattern alone, particularly if a smaller range of scan angles targeting calcium carbonates were used.

*S5. Additional statistics*

Since all temperature experiments represented pumping experiments without added B, $K_D$ values from pumping experiments without added B conducted at ~25 $^{o}$C were regressed against mean experimental saturation state and [$CO_3^{2-}$] (variations in [B] were too small to justify inclusion). The regressions gave the following fits: $K_D = -0.000865*\Omega + 0.0887$, $R^2 = 0.435$ and $K_D = 0.00000945*[CO_3^{2-}] + 0.0856$ $R^2 = 0.343$. Residuals ($K_D$ – calculated $K_D$) were then calculated for all pumping experiments without added boron and plotted against temperature (Fig. S3). There was no trend in residuals with temperature regardless of the regression used, thus suggesting any effect of temperature on $K_D$ is small relative to experimental variability. Equations 6 and 7 were also used for calculating the expected B/Ca ratio of each experiment, the difference between the measured and expected B/Ca ratio calculated, and again the values compared with temperature; no trend was detected. Tests for the effects of Tris, Hepes, and calcein were conducted in the same manner, regressions were calculated based on the full data-set (excluding experiments run in 2011, experiment 1c, and experiments containing Tris, Hepes, or calcein, (resulting equations: $K_D = 0.0997 -0.0111*[B] -0.00111*\Omega$ $R^2=0.53$, and $K_D = 0.0945 -0.0124*[B] -0.0000116*[CO_3^{2-}]$ $R^2=0.55$) residuals calculated and tested for significant ($p<0.01$) differences from 0 (t-test). In all cases, no significant differences were detected, though precipitates formed from solutions containing HEPES tended to have higher B/Ca than expected, while the opposite was observed for TRIS.

*S6. Effects of [Mg] and [Ca]*

Since our experiments were conducted over a wide range of Ca and Mg concentrations, departing substantially from standard seawater conditions, there is the potential for the seawater based carbonate chemistry constants used in the main text to be inappropriate for our data. The inclusion of seawater carbonate chemistry constants in common programs used for calculating carbonate chemistry leads to their application in modeling biogenic calcification, and thus our choice to use them, however both Ca and Mg influence DIC and B speciation (Reardon 1976; Bassett 1980; Hain et al., 2015), thus taking such effects into account is essential for a robust treatment of our data. We modified CO2Sys to use the DIC ($K_0$, $K_1$, $K_2$), boric acid ($K_B$), water ($K_W$), hydrogen sulfate ($K_{SO4}$), and aragonite solubility constants of Hain et al. (2015). We further modified the MyAMI code of Hain et al. (2015) used to calculate these constants to include variable $[H^+]$ (estimated from measured pH) and $[B(OH)_4^-]$ (estimated with CO2Sys without corrections for Mg and Ca) for estimating Pitzer activity coefficients. To estimate what parameters are likely to be affected by [Mg] and [Ca], we calculated concentrations of different DIC species and borate using constants from Hain et al (2015) at both normal seawater [Mg] and [Ca] and ~2x elevated (Fig. S5). For B/DIC the change in constants had no effect, while for $[B(OH)_4^-]/[CO_3^{2-}]^{0.5}$ there was a slight influence. In contrast many of the individual DIC or B species show substantial effects (Fig. S5, S6), thus the relationship between B/Ca and individual chemical species is likely to change. Correlations between B/Ca and various solution chemistry parameters are presented in Table S3 and Figure S7 (a summary table with all solution chemistry

parameters calculated using the adjusted constants is given in the supplemental data file). The use of different constants affected the correlations between B/Ca in the precipitate and some individual solution chemistry parameters (Table S3), however the strong correlations between B/Ca and mean $[B(OH)_4^-]/[CO_3^{2-}]^{0.5}$, [B]/[DIC] or $[B]/([CO_3^{2-}] + [HCO_3^-])$ and $[B(OH)_4^-]*[Ca^{2+}]$ remain consistent regardless of the constants used. Linear least squares regression (excluding experiment 1c for equations S1 and S2) using [Mg] and [Ca] corrected constants for solution chemistry calculations gave the following fits:

$$B/Ca\ (mmol/mol) = .0648\ (\pm 0.002)\ [B(OH)_4^-]/[CO_3^{2-}]^{0.5} + .0359\ (\pm 0.013) \quad \text{eq. S1}$$

$$B/Ca\ (mmol/mol) = 2.795\ (\pm 0.133)\ [B]/[DIC] + 0.089\ (\pm 0.014) \quad \text{eq. S2}$$

$$B/Ca\ (mmol/mol) = 0.000148\ (\pm 0.000009)\ [B(OH)_4^-]*[Ca^{2+}] + 0.0957\ (\pm 0.0178) \quad \text{eq. S3}$$

$$B/Ca\ (mmol/mol) = 0.001674\ (\pm 0.000144)\ [B(OH)_4^-] + 0.0799\ (\pm 0.0253) \quad \text{eq. S4}$$

where $[B(OH)_4^-]$, $[CO_3^{2-}]$, [B], and [DIC] are in units of μmol kg $sw^{-1}$, $[Ca^{2+}]$ is in mmol kg $sw^{-1}$ values in parentheses are 1 standard error, all parameter estimates were significant ($p \leq 0.001$, $R^2=0.93$ for eq. S1, $R^2=0.89$ for eq. S2, $R^2=0.82$ for eq. S3, and $R^2=0.71$ for eq. S4). Note that all coefficient estimates for eq. S1 and S2 are within one standard error of those in equations 4 and 5.

Apparent partition coefficients (relationships based on [B]/[DIC], $[B(OH)_4^-]$*/$[Ca^{2+}]$ and $[B(OH)_4^-]$ are not for balanced reactions) of the form K = (B/Ca)/solution chemistry value were calculated for each experiment as described in the main text (Table S4). The $K_D$ values based on $[B(OH)_4^-]/[CO_3^{2-}]^{0.5}$ thus calculated tend to be slightly higher than those calculated without taking the effects of $[Mg^{2+}]$ and $[Ca^{2+}]$ into account, reflecting slightly lower $[B(OH)_4^-]/[CO_3^{2-}]^{0.5}$ ratios (Fig. S5)

Although we consider a $K_D$ expression based on $[B(OH)_4^-]/[CO_3^{2-}]^{0.5}$ to provide the best fit to our data, involve species likely incorporated into aragonite, as well as providing a charge balanced reaction, there are a number of apparent partitioning relationships which fit our data nearly as well, some of which have been suggested to be important by other authors, thus we present alternative fits for $K_D$ relationships. For the following fits all solution chemistry parameters were calculated using [Ca] and [Mg] corrected constants, experiment 1c was excluded for relationships based on $[B(OH)_4^-]/[CO_3^{2-}]^{0.5}$ and [B]/DIC.

$K = B/Ca/[B(OH)_4^-]/[CO_3^{2-}]^{0.5} = -0.00008035\ (0.0000158)\ [B(OH)_4^-] + 0.0878\ (0.00278)$, $R^2=0.32$ eq. S5

$K = B/Ca/[B(OH)_4^-]/[CO_3^{2-}]^{0.5} = -0.00001634\ (0.00000276)\ [CO_3^{2-}] - 0.00001062\ (0.00000177)\ [B] + 0.104\ (0.004)$, $R^2=0.49$ eq. S6

$K = B/Ca/[B(OH)_4^-]/[CO_3^{2-}]^{0.5} = -0.001243\ (0.0002)\ \Omega\ -0.00001065\ (0.00000173)\ [B] +$ $0.1072\ (0.00457),\ R^2=0.51$ eq. S7

$K = B/Ca/[B]/DIC = -0.005306\ (0.001164)\ [B(OH)_4^-] - 0.214\ (0.0275)\ [Ca^{2+}] + 7.356$ $(0.385),\ R^2=0.57$ eq. S8

$K = B/Ca/[B(OH)_4^-]*[Ca^{2+}] = -0.0000117\ (0.00000114)\ [Ca^{2+}] - 0.00000776$ $(0.00000059)\ \Omega\ -\ 0.0000000462\ (0.00000000488)\ [B] + 0.000535\ (0.0000197),\ R^2 = 0.87$ eq. S9

$K = B/Ca/[B(OH)_4^-] = -0.000001377\ (0.000000097)\ [CO_3^{2-}] - 0.0000003825$ $(0.000000062)\ [B] + 0.00433\ (0.00015),\ R^2 = 0.79$ eq S10

where $[B(OH)_4^-]$, $[CO_3^{2-}]$, [B], and [DIC] are in units of μmol kg $sw^{-1}$, $[Ca^{2+}]$ is in mmol kg $sw^{-1}$ values in parentheses are 1 standard error, all parameter estimates were significant ($p \leq 0.001$). B/Ca ratios were calculated based on each of the above $K_D$ expressions and compared to measured values (Table S5). Equations S6, S7, and S9 provided the best fits. Residuals showed no significant effect of TRIS; for HEPES measured values were significantly ($p<0.01$) higher than expected based on equation S9. Residuals from equation S8 were negatively correlated with temperature, whereas residuals from equations S3 and S4 were weakly positively correlated with temperature.

Although in the full data set the correlation between B/Ca in the precipitate and $[B(OH)_4^-]*[Ca^{2+}]$ was nearly equivalent to correlations with $[B(OH)_4^-]/[CO_3^{2-}]^{0.5}$ and

[B]/DIC, when data were separated by pumping vs degassing experiments, the use of $[B(OH)_4^-]*[Ca^{2+}]$ provided no improvement in the correlation relative to $[B(OH)_4^-]$ alone (e.g. Table 1). In contrast, $[B(OH)_4^-]/[CO_3^{2-}]^{0.5}$ was consistently more strongly correlated with B/Ca than $[B(OH)_4^-]$ alone. This suggests that rather than $[Ca^{2+}]$ being important in and of itself, it reflects a difference amongst degassing versus pumping experiments. Indeed $[Ca^{2+}]$ was generally higher in degassing experiments, while carbonate was generally lower (relative to pumping experiments) leading to a negative correlation between $[CO_3^{2-}]$ and $[Ca^{2+}]$ in both the overall data-set and certain subsets of the data. Thus we consider the strong correlation of B/Ca with $[B(OH)_4^-]*[Ca^{2+}]$ to reflect $[B(OH)_4^-]$ and a negative correlation between $[Ca^{2+}]$ and $[CO_3^{2-}]$ rather than an effect of $[Ca^{2+}]$.

## Supplemental References


**Bassett RL. 1980.** A critical evaluation of the thermodynamic data for boron ions, ion pairs, complexes, and polyanions in aqueous solution at 298.15 K and 1 bar. Geochimica et Cosmochimica Acta **44**:1151-1160 http://dx.doi.org/10.1016/0016-7037(80)90069-1.

**Dickson AG. 1993.** pH buffers for sea water media based on the total hydrogen ion concentration scale. Deep-Sea Research **40**:107-118

**Dickson AG, Millero FJ. 1987.** A comparison of the equilibrium constants for the dissociation of carbonic acid in seawater media. Deep-Sea Research **34**:1733-1743

**Dickson AG, Wesolowski DJ, Palmer DA, Mesmer RE. 1990.** Dissociation constant of bisulfate ion in aqueous sodium chloride solutions to 250.degree.C. The Journal of Physical Chemistry **94**:7978-7985 10.1021/j100383a042.

**Dissard D, Douville E, Reynaud S, Juillet-Leclerc A, Montagna P, Louvat P, McCulloch M. 2012.** Light and temperature effect on d11B and B/Ca ratios of the zooxanthellate coral

*Acropora sp.*: results from culturing experiments. Biogeosciences Discussions **9**:5969-6014 10.5194/bgd-9-5969-2012.

**Fofonoff N. 1985.** Physical Properties of Seawater A New Salinity Scale and Equation of State for Seawater. Journal of Geophysical Research **90**:3332-3342

**Foster GL, Ni Y, Haley B, Elliott T. 2006.** Accurate and precise isotopic measurement of sub-nanogram sized samples of foraminiferal hosted boron by total evaporation NTIMS. Chemical Geology **230**:161-174 http://dx.doi.org/10.1016/j.chemgeo.2005.12.006.

**Holcomb M, McCorkle DC, Cohen AL. 2010.** Long-term effects of nutrient and CO2 enrichment on the temperate coral Astrangia poculata (Ellis and Solander, 1786). J Exp Mar Biol Ecol **386**:27-33

**Holcomb M, Cohen AL, McCorkle DC. 2012.** An investigation of the calcification response of the scleractinian coral *Astrangia poculata* to elevated pCO2 and the effects of nutrients, zooxanthellae and gender. Biogeosciences **9**:29-39 10.5194/bg-9-29-2012.

**Holcomb M, Rankenburg K, McCulloch M. 2014.** High Precision MC-ICP-MS measurements of δ11B: matrix effects in direct injection and spray chamber sample introduction systems. . In: Grice, K (Ed), Principles and Practice of Analytical Techniques in Geosciences Royal Society of Chemistry, England, pp 251–270

**Holcomb M, DeCarlo TM, Schoepf V, Dissard D, Tanaka K, McCulloch M. 2015.** Cleaning and pre-treatment procedures for biogenic and synthetic calcium carbonate powders for determination of elemental and boron isotopic compositions. Chemical Geology **398**:11-21 http://dx.doi.org/10.1016/j.chemgeo.2015.01.019.

**Lécuyer C, Grandjean P, Reynard B, Albarède F, Telouk P. 2002.** 11B/10B analysis of geological materials by ICP–MS Plasma 54: Application to the boron fractionation between brachiopod calcite and seawater. Chemical Geology **186**:45-55 http://dx.doi.org/10.1016/S0009-2541(01)00425-9.

**Lee K, Kim T-W, Byrne RH, Millero FJ, Feely RA, Liu Y-M. 2010.** The universal ratio of boron to chlorinity for the North Pacific and North Atlantic oceans. Geochimica et Cosmochimica Acta **74**:1801-1811 10.1016/j.gca.2009.12.027.

**Lemarchand D, Gaillardet J, Göpel C, Manhès G. 2002.** An optimized procedure for boron separation and mass spectrometry analysis for river samples. Chemical Geology **182**:323-334 http://dx.doi.org/10.1016/S0009-2541(01)00329-1.

**McCulloch MT, Holcomb M, Rankenburg K, Trotter JA. 2014.** Rapid, high-precision measurements of boron isotopic compositions in marine carbonates. Rapid Communications in Mass Spectrometry **28**:2704-2712 10.1002/rcm.7065.

**Mehrbach C, Culberson CH, Hawley JE, Pytkowicz RM. 1973.** Measurement of the apparent dissociation constants of carbonic acid in seawater at atmospheric pressure. Limnology and Oceanography **18**:897-907

**Pawlowicz R. 2010.** A model for predicting changes in the electrical conductivity, practical salinity, and absolute salinity of seawater due to variations in relative chemical composition. Ocean Sci **6**:361-378 10.5194/os-6-361-2010.

**Reardon EJ. 1976.** Dissociation constants for alkali earth and sodium borate ion pairs from 10 to 50℃. Chemical Geology **18**:309-325 http://dx.doi.org/10.1016/0009-2541(76)90013-9.

**Trotter J, Montagna P, McCulloch M, Silenzi S, Reynaud S, Mortimer G, Martin S, Ferrier-Pagès C, Gattuso J-P, Rodolfo-Metalpa R. 2011.** Quantifying the pH 'vital effect' in the temperate zooxanthellate coral *Cladocora caespitosa*: Validation of the boron seawater pH proxy. Earth and Planetary Science Letters **303**:163-173 10.1016/j.epsl.2011.01.030.

**Zinke J, Rountrey A, Feng M, Xie SP, Dissard D, Rankenburg K, Lough JM, McCulloch MT. 2014.** Corals record long-term Leeuwin current variability including Ningaloo Niño/Niña since 1795. Nat Commun **5**10.1038/ncomms4607.

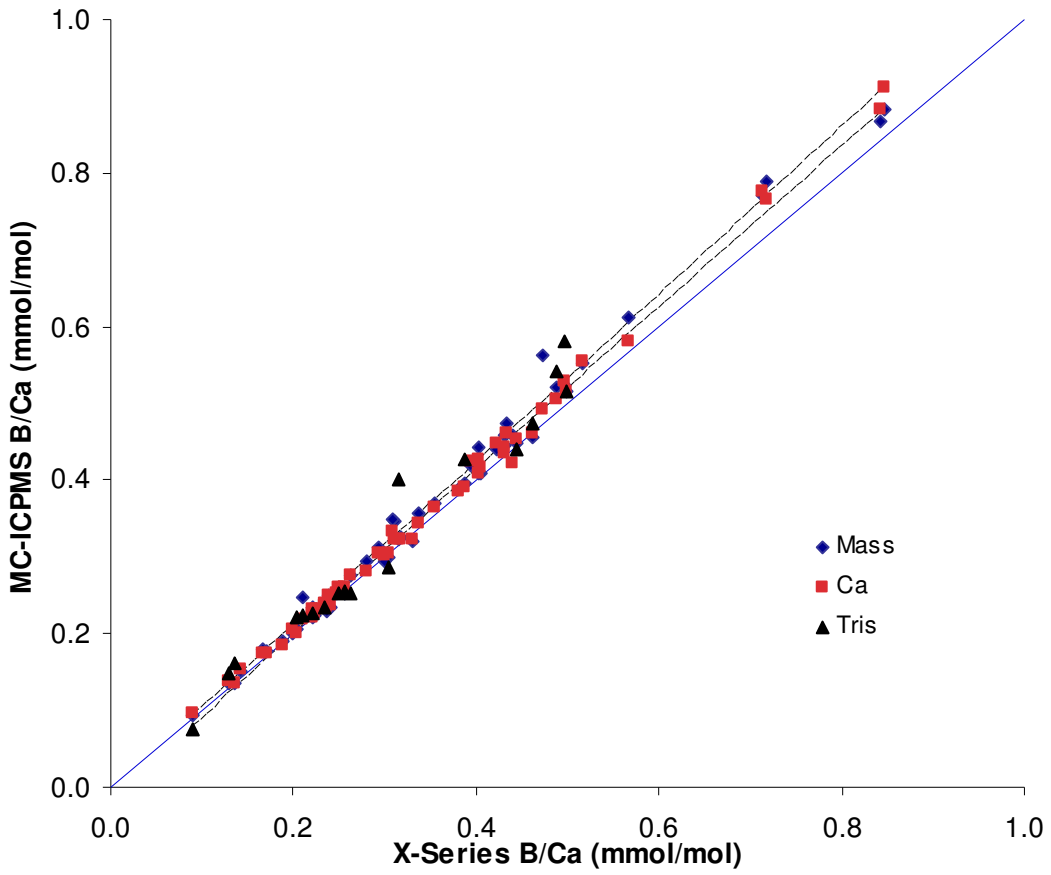


Figure S1. Relationship between different methods of determining B/Ca ratios. B/Ca ratios measured on the X-Series are plotted on the x-axis versus measurements made via MC-ICPMS (y-axis). Samples for which B (measured via MC-ICPMS) was extracted using column chemistry were normalized to Ca based on sample mass (blue diamonds), or measured Ca contents (red-orange squares). Samples for which B was extracted using Amberlite resin and TRIS buffer were normalized to Ca based on sample mass (black triangles). The 1:1 line is shown for reference (blue line). The relationship between the X-series measurements and MC-ICPMS measurements (normalized based on sample mass) was described by the following linear regression: B/Ca MC-ICPMS = B/Ca X-series *1.07 – 0.009 ($R^2$=0.99); the 95% confidence intervals for this regression are shown as dashed lines.

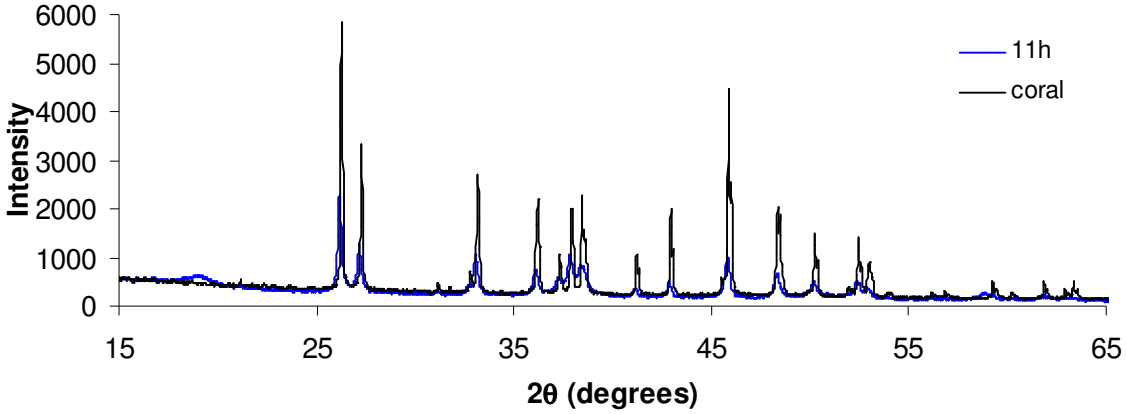


Fig S2. XRD patterns of a coral aragonite powder (black) and synthetic precipitate 11h (blue) containing a Mg rich phase in addition to aragonite.

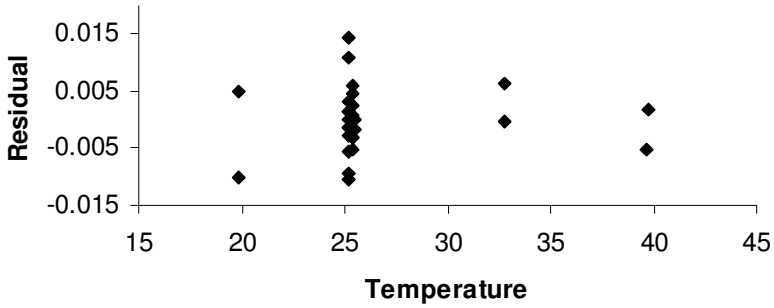


Figure S3. Residuals (experimental $K_D$ – $K_D$ calculated from $K_D$ = -0.000865*Ω +0.0887) plotted versus temperature for pumping experiments without added B.

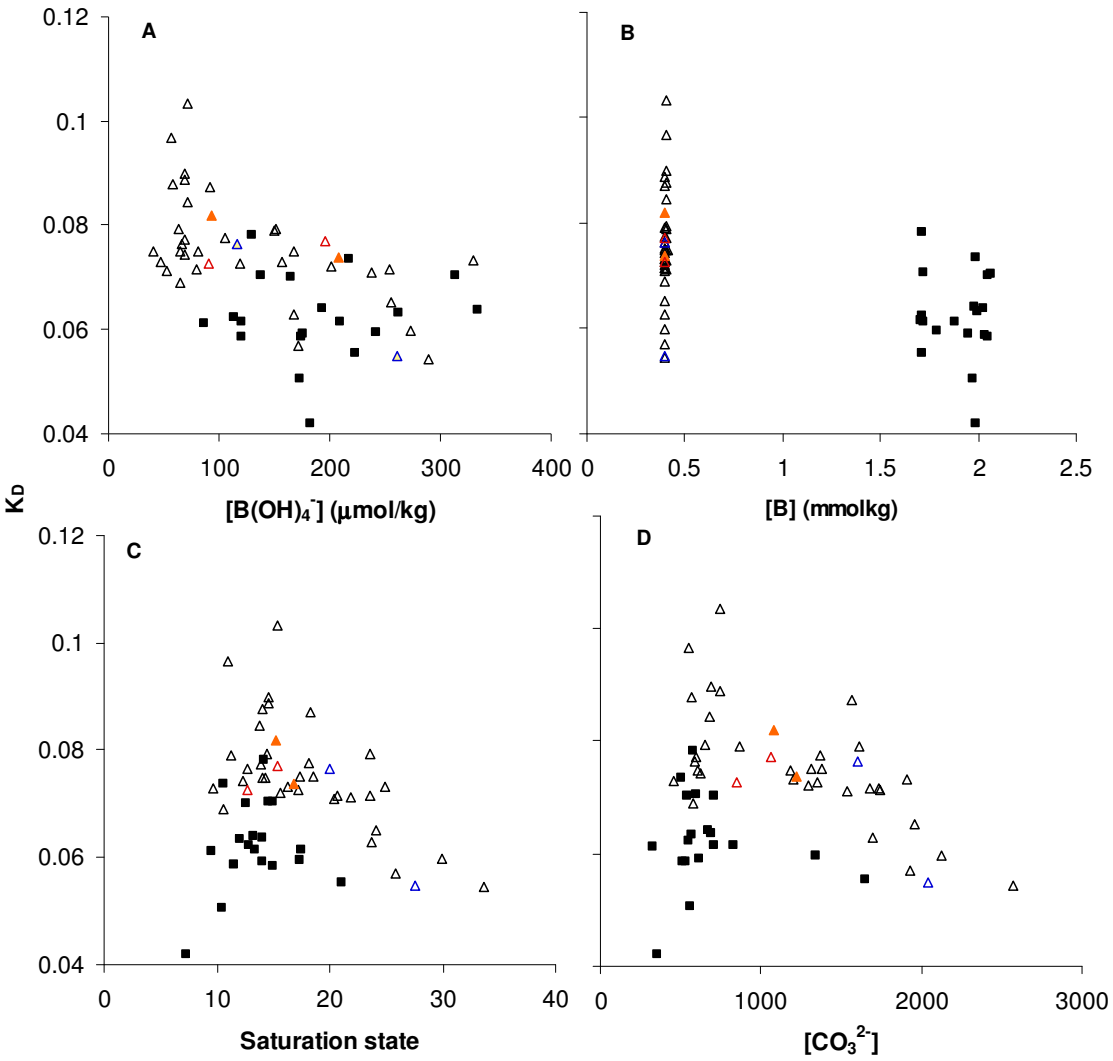


1366

1367 Figure S4. Relationship between different solution chemistry parameters and $K_D$.

1368 Symbols are means of individual experiments; experiments without added B are

1369 represented by triangles, experiments with added B are represented by squares, error bars

1370 are omitted for clarity. Experiments conducted at different temperatures are shown in

1371 different colors: blue ~ 20, black ~ 25, orange ~ 33, and red ~ 40 $^{o}$C. Most experiments

1372 were conducted at ~ 25 $^{o}$C, 2 experiments were run at each of the other temperatures.

1373

1374

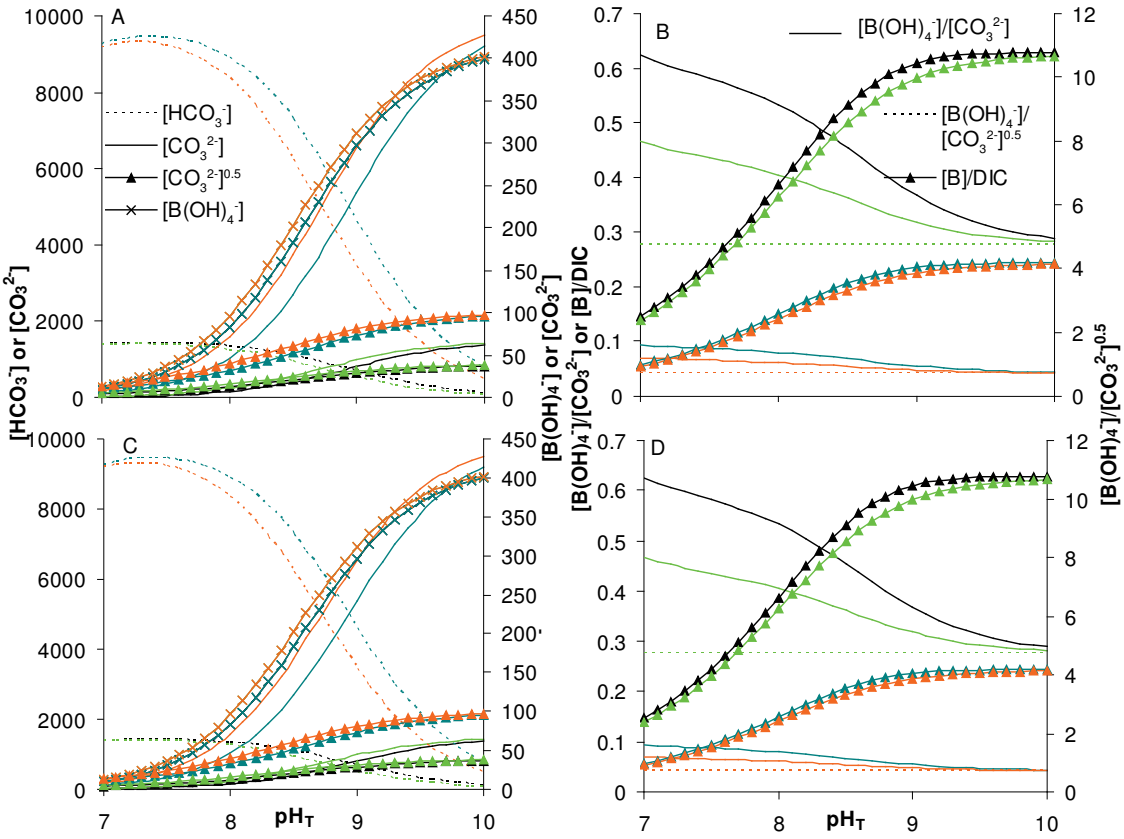


1375
1376 Figure S5. Relationships amongst DIC species as a function of pH calculated using
1377 constants from Hain et al. (2015). In A and B, two different DIC levels are used (1500 =
1378 black and green, 10000 = blue and orange); for each DIC, carbonate chemistry constants
1379 are calculated using the Pitzer model from the MyAMI code under standard seawater
1380 [Ca] and [Mg] (black and blue) or 2x [Ca] and [Mg] (green and orange). In C and D the
1381 same calculations are made but with additional corrections for the effects of pH
1382 variations on ion activity coefficients.

1383

1384

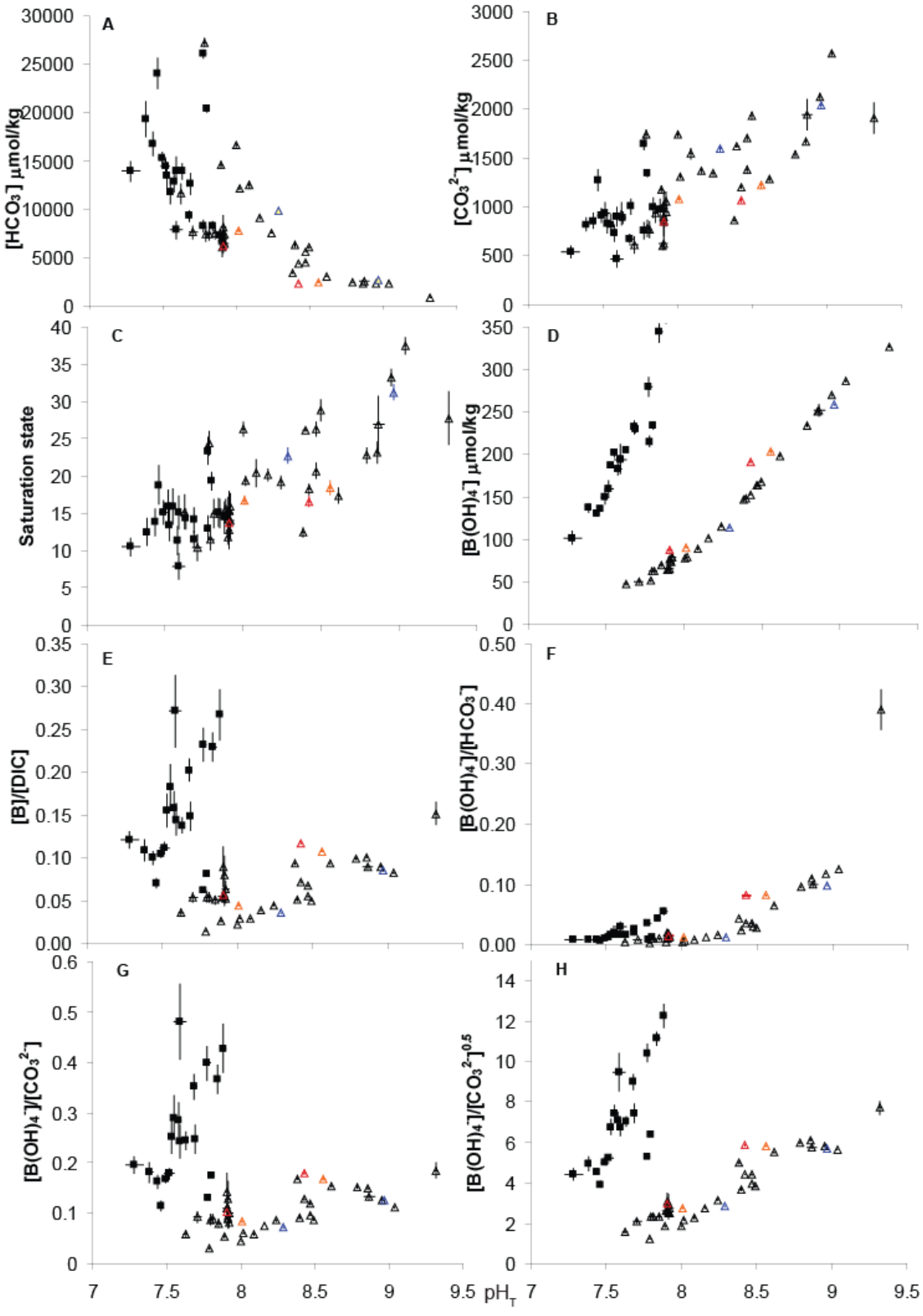
A
B
C
D
E
F
G
H
[HCO3] µmol/kg
[CO3 2] µmol/kg
Saturation state
[B(OH)4] µmol/kg
[B]/[DIC]
[B(OH)4]/[HCO3]
[B(OH)4]/[CO3 2]
[B(OH)4]/[CO3 2]0.5
pHT

1385

Figure S6. Relationship between different solution chemistry parameters and $pH_T$ as calculated using [Mg] and [Ca] corrected constants from Hain et al. (2015). Symbols are means of individual experiments; experiments without added B are represented by triangles, experiments with added B are represented by squares, lines show bi-direction error bars (1 sd). Experiments conducted at different temperatures are shown in different colors: blue ~ 20, black ~ 25, orange ~ 33, and red ~ 40 $^{o}$C. Most experiments were conducted at ~ 25 $^{o}$C, 2 experiments were run at each of the other temperatures.

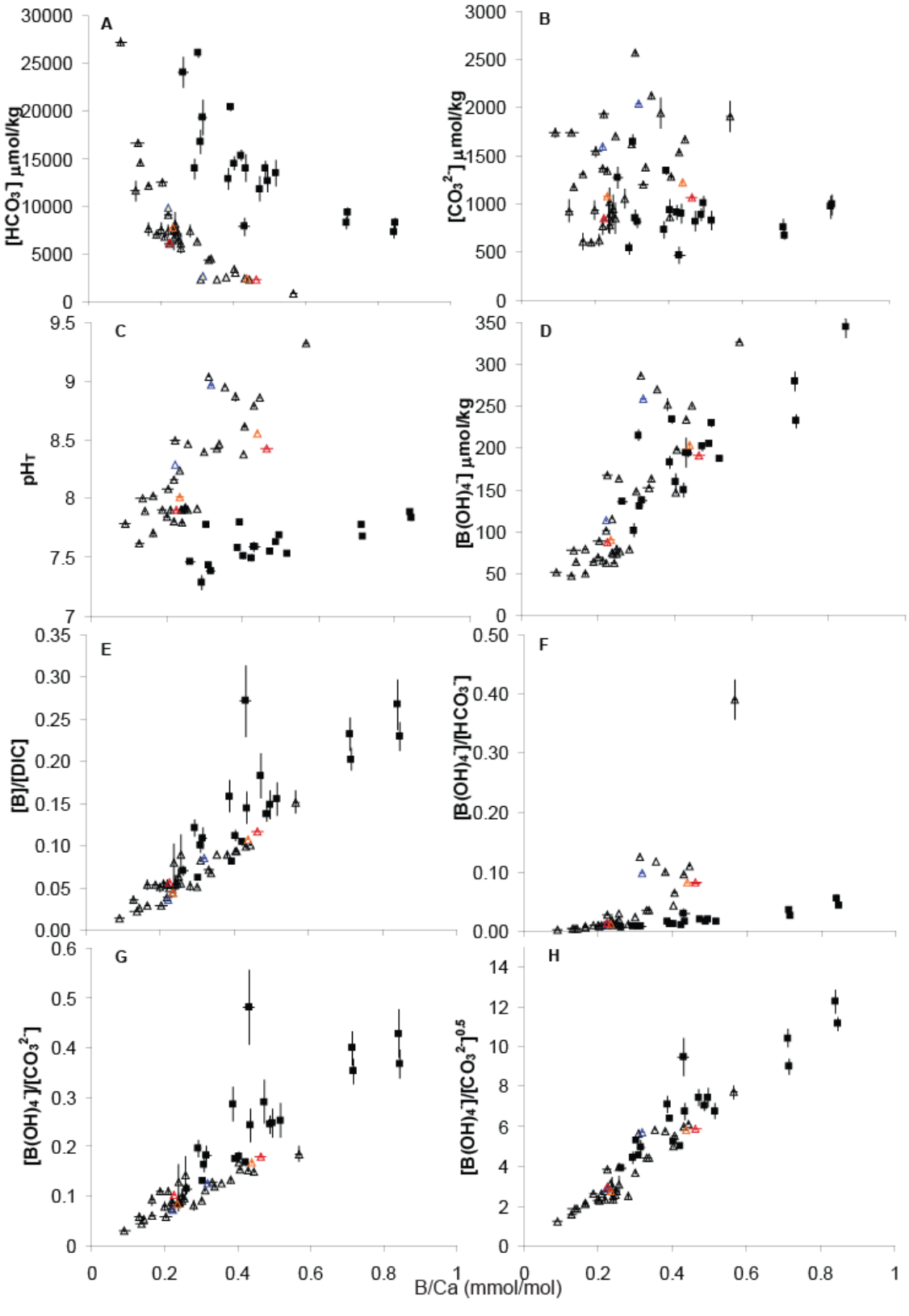


1393

1394 Figure S7. Relationship between B/Ca (mmol/mol) in aragonite and various solution

chemistry parameters. Units for all species in solution are μmol/kg sw. Symbols are as described for Figure S6.

1399 Table S1. Experiment name, general description of precipitation approach used and any

1400 organic additives added. All experiments were carried out at 25 – 25.5 $^{o}$C unless

1401 specified otherwise. Those carried out at ~20 $^{o}$C are highlighted in blue, ~33 $^{o}$C in

1402 orange, ~40 $^{o}$C in red.

| Experiment name/ precipitate | Description | Additives |
|---|---|---|
| 1/19/11 a | Degassing, bubbled with air | calcein, OTC, alizarin |
| 1/19/11 c | Degassing, bubbled with air | calcein |
| 1/19/11 d | Degassing, bubbled with air | |
| 1/19/11 f | Degassing, bubbled with air | |
| 1/20/11 1 | Pumping with $Na_2CO_3$ | calcein, OTC |
| 1/20/11 2 | Pumping with $Na_2CO_3$ | |
| 1a | Degassing | |
| 1c | Degassing with added B | |
| 1e | Degassing with added B | TRIS |
| 1f | Pumping with $Na_2CO_3$ | |
| 1g | Pumping with $Na_2CO_3$ | |
| 1h / ts20 | Pumping with $Na_2CO_3$ | |
| 2a / ts9 | Degassing, bubbled with air | |
| 2b / ts8 | Degassing, bubbled with air, added $CaCl_2$ | |
| 2c / ts6 | Degassing, bubbled with air, added B | |
| 2d / ts11 | Degassing, bubbled with air, added B | HEPES |
| 2e / ts5 | Degassing, bubbled with air, added B | TRIS |
| 2f / ts10 | Pumping with $Na_2CO_3$/$NaHCO_3$, $Na_2CO_3$ during precipitation | |
| 2g / ts1 | Pumping with $Na_2CO_3$/$NaHCO_3$ | |
| 2h / ts2 | Pumping with $Na_2CO_3$, 20 $^{o}$C | |
| 3a / ts19 | Degassing, bubbled with air | |
| 3b / ts16 | Degassing, bubbled with air | |
| 3c / ts18 | Degassing, bubbled with air, added B | |
| 3d / ts17 | Degassing, bubbled with air, added B | |
| 3e / ts15 | Degassing, bubbled with air, added B | TRIS |
| 3f / ts12 | Pumping with $Na_2CO_3$ | |
| 3g / ts3 | Pumping with $Na_2CO_3$/$NaHCO_3$, $Na_2CO_3$ during precipitation | |
| 3h | Pumping with $Na_2CO_3$, 33 $^{o}$C | |
| 4a / ts26 | Degassing, bubbled with air | |
| 4b / ts33 | Degassing, bubbled with air, added $CaCl_2$ | |
| 4c / ts28 | Degassing, bubbled with air, added $CaCl_2$ | |
| 4d / ts29 | Degassing, bubbled with air, added $Na_2CO_3$ and 2xsw | |

| | | |
|---|---|---|
| 4e / ts32 | Degassing, bubbled with air, added $Na_2CO_3$ | |
| 4f / ts22 | Pumping with $NaHCO_3$, $Na_2CO_3$ during precipitation | |
| 4g / ts4 | Pumping with $Na_2CO_3$/$NaHCO_3$, $Na_2CO_3$ during precipitation | |
| 5a / ts41 | Degassing, bubbled with ~5000 ppmv $CO_2$ | |
| 5b / ts39 | Degassing, bubbled with ~5000 ppmv $CO_2$, added $Na_2CO_3$ and B | |
| 5c / ts40 | Degassing, bubbled with ~5000 ppmv $CO_2$, added $CaCl_2$ and B | |
| 5d / ts42 | Degassing, bubbled with ~5000 ppmv $CO_2$, added B | HEPES |
| 5e / ts38 | Degassing, bubbled with ~5000 ppmv $CO_2$, added B | TRIS |
| 5f / ts24 | Pumping with $Na_2CO_3$ | |
| 5g / ts14 | Pumping with $NaHCO_3$, $Na_2CO_3$ during precipitation | |
| 5h / ts7 | Pumping with $Na_2CO_3$, 40 $^oC$ | |
| 6a / ts54 | Degassing, bubbled with ~15000 ppmv $CO_2$, added B | |
| 6b / ts49 | Degassing, bubbled with ~15000 ppmv $CO_2$, added $CaCl_2$ and B | |
| 6c / ts52 | Degassing, bubbled with ~15000 ppmv $CO_2$, added $NaHCO_3$ and B | |
| 6d | Degassing, bubbled with ~15000 ppmv $CO_2$, added B | HEPES |
| 6e / ts43 | Degassing, bubbled with ~15000 ppmv $CO_2$, added B | TRIS |
| 6f / ts50 | Pumping with $Na_2CO_3$ | |
| 6g / ts23 | Pumping with $NaHCO_3$, $Na_2CO_3$ during precipitation | |
| 6h / ts13 | Pumping with $NaHCO_3$, $Na_2CO_3$ during precipitation, 40 $^oC$ | |
| 7g / ts25 | Pumping with $NaHCO_3$, $Na_2CO_3$ during precipitation | |
| 7h / ts21 | Pumping with $NaHCO_3$, $Na_2CO_3$ during precipitation, 33 $^oC$ | |
| 8f / ts44 | Pumping with seawater containing $CaCO_3$ and $SrCO_3$ (dissolved with $CO_2$), bubbled with air | |
| 8g / ts27 | Pumping with $Na_2CO_3$/$NaHCO_3$, $Na_2CO_3$ during precipitation | |
| 8h / ts31 | Pumping with $NaHCO_3$, $Na_2CO_3$ during precipitation, 20 $^oC$ | |

| | | |
|---|---|---|
| 9g / ts30 | Pumping with $NaHCO_3$, $Na_2CO_3$ during precipitation | |
| 9h / ts37 | Pumping with $NaHCO_3$, $Na_2CO_3$ during precipitation, bubbled with ~5000 ppmv $CO_2$ | |
| 10g / ts36 | Pumping with $NaHCO_3$, $Na_2CO_3$ during precipitation, bubbled with ~2000 ppmv $CO_2$ | |
| 10h / ts45 | Pumping with $NaHCO_3$, $Na_2CO_3$ during precipitation, added B | |
| 11g / ts46 | Pumping with $NaHCO_3$, $Na_2CO_3$ during precipitation, added B, bubbled with ~15 000 ppmv $CO_2$ | |
| 11h / ts48 | Pumping with $Na_2CO_3$/NaOH | |
| 12g / ts51 | Pumping with $Na_2CO_3$ | calcein |
| 13g / ts53 | Pumping with seawater containing $CaCO_3$ and $SrCO_3$ (dissolved with $CO_2$), bubbled with air | |
| 13h / ts47 | Pumping with $Na_2CO_3$/NaOH | |

1403

Table S2. Summary of experimental chemistry during precipitation, B/Ca ratios in the precipitate, and $K_D$ values. The standard deviation for solution chemistry values is given in the corresponding "sd" column. Experiments performed at different temperatures are in different colors: blue ~20 $^oC$, black ~25 $^oC$, orange ~33 $^oC$, and red ~40 $^oC$. TA, $pH_T$, and B/Ca (X-Series measurement) were measured, other values were calculated. For a subset of experiments B was also measured (see supplemental .xls file).

| Exp. | $pH_T$ | sd | TA (µmol/kg) | sd | TC (µmol/kg) | sd | $HCO_3^-$ (µmol/kg) | sd | $CO_3^{2-}$ (µmol/kg) | sd | $\Omega_{Arag}$ | sd | B (mmol/kg) | sd | Borate (µmol/kg) | sd | B/Ca (mmol/mol) | Kd |
|---|---|---|---|---|---|---|---|---|---|---|---|---|---|---|---|---|---|---|
| 1/19/11a | 7.72 | 0.05 | 11575 | 1914 | 11103 | 1862 | 10376 | 1752 | 573 | 96 | 13.4 | 3.2 | 0.404 | 0.000 | 49 | 5 | 0.22 | 0.097 |
| 1/19/11c | 7.61 | 0.05 | 11684 | 2057 | 11401 | 2038 | 10740 | 1933 | 450 | 74 | 10.5 | 2.5 | 0.405 | 0.000 | 39 | 5 | 0.16 | 0.080 |
| 1/19/11d | 7.78 | 0.04 | 11358 | 1961 | 10794 | 1881 | 10033 | 1753 | 633 | 118 | 15.0 | 3.8 | 0.402 | 0.000 | 54 | 5 | 0.21 | 0.087 |
| 1/19/11f | 7.64 | 0.05 | 11586 | 2066 | 11268 | 2054 | 10605 | 1953 | 468 | 64 | 10.8 | 2.2 | 0.405 | 0.000 | 42 | 5 | 0.18 | 0.085 |
| 1/20/11-1 | 8.33 | 0.04 | 4282 | 176 | 3486 | 86 | 2819 | 47 | 656 | 86 | 8.6 | 1.6 | 0.395 | 0.001 | 136 | 9 | 0.62 | 0.115 |
| 1/20/11-2 | 8.34 | 0.06 | 4015 | 129 | 3248 | 57 | 2614 | 76 | 624 | 80 | 8.4 | 1.4 | 0.395 | 0.000 | 138 | 12 | 0.58 | 0.105 |
| 1a | 7.71 | 0.03 | 8890 | 808 | 8491 | 758 | 7924 | 696 | 458 | 64 | 9.6 | 1.6 | 0.403 | 0.000 | 47 | 3 | 0.17 | 0.073 |

| | | | | | | | | | | | | | | | | | | |
|---|---|---|---|---|---|---|---|---|---|---|---|---|---|---|---|---|---|---|
| 1c | 7.59 | 0.04 | 8992 | 1049 | 8609 | 1015 | 8105 | 950 | 351 | 64 | 7.3 | 1.7 | 1.988 | 0.001 | 183 | 16 | 0.43 | 0.042 |
| 1e | 7.58 | 0.02 | 20294 | 1313 | 14021 | 1179 | 13222 | 1105 | 555 | 62 | 10.5 | 1.7 | 1.970 | 0.000 | 173 | 7 | 0.39 | 0.051 |
| 1f | 8.61 | 0.01 | 5826 | 54 | 4313 | 36 | 3017 | 22 | 1291 | 19 | 15.6 | 0.9 | 0.400 | 0.000 | 202 | 1 | 0.41 | 0.072 |
| 1g | 8.79 | 0.01 | 5813 | 65 | 3999 | 40 | 2454 | 20 | 1542 | 25 | 20.4 | 1.0 | 0.396 | 0.000 | 238 | 1 | 0.43 | 0.071 |
| 1h | 8.86 | 0.01 | 5907 | 73 | 3932 | 44 | 2251 | 19 | 1679 | 28 | 20.7 | 1.3 | 0.397 | 0.000 | 254 | 1 | 0.44 | 0.072 |
| 2a | 7.91 | 0.01 | 9152 | 852 | 8456 | 789 | 7703 | 714 | 687 | 71 | 14.5 | 1.9 | 0.404 | 0.000 | 69 | 1 | 0.25 | 0.090 |
| 2b | 7.81 | 0.01 | 9019 | 784 | 8475 | 732 | 7826 | 669 | 565 | 59 | 14.0 | 1.8 | 0.404 | 0.000 | 57 | 1 | 0.22 | 0.088 |
| 2c | 7.77 | 0.02 | 10045 | 754 | 9311 | 699 | 8639 | 638 | 570 | 62 | 12.1 | 1.7 | 1.994 | 0.000 | 263 | 11 | 0.71 | 0.063 |
| 2d | 7.68 | 0.02 | 16782 | 778 | 10312 | 624 | 9663 | 588 | 508 | 33 | 10.6 | 1.0 | 1.990 | 0.000 | 217 | 7 | 0.72 | 0.074 |
| 2e | 7.63 | 0.00 | 22300 | 915 | 15281 | 905 | 14377 | 852 | 668 | 39 | 13.2 | 1.2 | 1.977 | 0.000 | 194 | 2 | 0.49 | 0.064 |
| 2f | 8.47 | 0.01 | 7492 | 100 | 5936 | 71 | 4544 | 48 | 1381 | 32 | 18.5 | 0.9 | 0.398 | 0.000 | 167 | 2 | 0.34 | 0.075 |
| 2g | 8.40 | 0.01 | 9715 | 270 | 7956 | 253 | 6327 | 231 | 1611 | 23 | 23.6 | 0.2 | 0.399 | 0.000 | 152 | 2 | 0.30 | 0.079 |
| 2h | 8.96 | 0.00 | 7034 | 62 | 4700 | 40 | 2656 | 19 | 2041 | 22 | 27.6 | 1.0 | 0.397 | 0.001 | 261 | 1 | 0.32 | 0.055 |
| 3a | 7.92 | 0.01 | 9615 | 843 | 8855 | 784 | 8038 | 712 | 750 | 67 | 15.4 | 1.8 | 0.406 | 0.000 | 72 | 1 | 0.28 | 0.103 |
| 3b | 7.79 | 0.02 | 9040 | 893 | 8521 | 852 | 7885 | 791 | 547 | 55 | 11.0 | 1.5 | 0.406 | 0.000 | 56 | 2 | 0.24 | 0.097 |
| 3c | 7.88 | 0.02 | 9597 | 844 | 8637 | 763 | 7875 | 681 | 691 | 80 | 14.0 | 2.0 | 2.022 | 0.000 | 334 | 11 | 0.84 | 0.064 |
| 3d | 7.84 | 0.02 | 10623 | 705 | 9689 | 632 | 8897 | 562 | 704 | 72 | 14.5 | 1.8 | 2.063 | 0.000 | 313 | 12 | 0.85 | 0.070 |
| 3e | 7.69 | 0.01 | 21855 | 1166 | 14118 | 1241 | 13218 | 1170 | 709 | 51 | 13.3 | 1.5 | 1.877 | 0.000 | 209 | 4 | 0.50 | 0.061 |

| | | | | | | | | | | | | | | | | | | |
|---|---|---|---|---|---|---|---|---|---|---|---|---|---|---|---|---|---|---|
| 3f | 8.95 | 0.01 | 6876 | 67 | 4426 | 34 | 2299 | 3 | 2124 | 32 | 29.9 | 1.0 | 0.396 | 0.000 | 273 | 1 | 0.35 | 0.060 |
| 3g | 8.43 | 0.00 | 6976 | 61 | 5614 | 46 | 4400 | 32 | 1201 | 17 | 16.3 | 0.6 | 0.397 | 0.000 | 157 | 1 | 0.33 | 0.073 |
| 3h | 8.56 | 0.01 | 5174 | 63 | 3708 | 35 | 2484 | 11 | 1220 | 27 | 16.9 | 0.9 | 0.398 | 0.000 | 208 | 2 | 0.44 | 0.074 |
| 4a | 7.92 | 0.02 | 8452 | 945 | 7750 | 851 | 7011 | 751 | 681 | 102 | 13.7 | 2.5 | 0.405 | 0.000 | 72 | 3 | 0.25 | 0.085 |
| 4b | 7.90 | 0.00 | 7884 | 1337 | 7268 | 1243 | 6614 | 1130 | 597 | 104 | 13.9 | 2.7 | 0.405 | 0.000 | 69 | 0 | 0.26 | 0.077 |
| 4c | 7.85 | 0.01 | 9536 | 819 | 8894 | 760 | 8161 | 690 | 654 | 67 | 14.4 | 1.9 | 0.406 | 0.000 | 63 | 2 | 0.20 | 0.079 |
| 4d | 7.91 | 0.02 | 10246 | 1522 | 9502 | 1442 | 8677 | 1332 | 748 | 98 | 14.6 | 2.6 | 0.397 | 0.000 | 69 | 3 | 0.24 | 0.089 |
| 4e | 7.91 | 0.02 | 8433 | 1503 | 7802 | 1412 | 7118 | 1294 | 620 | 106 | 12.4 | 2.5 | 0.400 | 0.000 | 69 | 2 | 0.24 | 0.074 |
| 4f | 8.16 | 0.00 | 11956 | 136 | 10522 | 122 | 9111 | 107 | 1365 | 15 | 18.1 | 0.7 | 0.398 | 0.000 | 105 | 0 | 0.22 | 0.078 |
| 4g | 8.47 | 0.00 | 9161 | 83 | 7294 | 64 | 5586 | 48 | 1695 | 21 | 23.6 | 0.9 | 0.398 | 0.000 | 167 | 1 | 0.26 | 0.063 |
| 5a | 7.62 | 0.01 | 13509 | 1317 | 13058 | 1258 | 12258 | 1172 | 604 | 72 | 14.3 | 2.2 | 0.412 | 0.000 | 41 | 1 | 0.13 | 0.075 |
| 5b | 7.59 | 0.01 | 16006 | 1586 | 15475 | 1555 | 14594 | 1468 | 617 | 61 | 14.1 | 2.0 | 1.949 | 0.000 | 175 | 3 | 0.43 | 0.059 |
| 5c | 7.55 | 0.01 | 13669 | 1460 | 13217 | 1419 | 12466 | 1336 | 513 | 61 | 14.9 | 2.2 | 2.050 | 0.000 | 174 | 3 | 0.47 | 0.059 |
| 5d | 7.53 | 0.01 | 19533 | 1550 | 14885 | 1476 | 14061 | 1393 | 537 | 57 | 12.5 | 1.9 | 2.046 | 0.000 | 164 | 2 | 0.52 | 0.070 |
| 5e | 7.38 | 0.02 | 25217 | 1844 | 21058 | 1981 | 19938 | 1877 | 531 | 39 | 11.5 | 1.6 | 2.032 | 0.000 | 121 | 5 | 0.32 | 0.059 |
| 5f | 9.04 | 0.00 | 7783 | 50 | 4855 | 25 | 2281 | 6 | 2573 | 24 | 33.7 | 1.1 | 0.397 | 0.000 | 290 | 1 | 0.31 | 0.054 |
| 5g | 8.02 | 0.00 | 14910 | 180 | 13591 | 171 | 12194 | 160 | 1314 | 14 | 17.4 | 0.6 | 0.398 | 0.000 | 81 | 1 | 0.17 | 0.075 |
| 5h | 8.43 | 0.01 | 4718 | 33 | 3406 | 20 | 2335 | 14 | 1066 | 14 | 15.3 | 0.7 | 0.399 | 0.000 | 196 | 1 | 0.46 | 0.077 |

| | | | | | | | | | | | | | | | | | | |
|---|---|---|---|---|---|---|---|---|---|---|---|---|---|---|---|---|---|---|
| 6a | 7.52 | 0.03 | 16546 | 884 | 16130 | 809 | 15220 | 747 | 593 | 68 | 14.9 | 2.1 | 1.724 | 0.000 | 138 | 9 | 0.40 | 0.071 |
| 6b | 7.28 | 0.06 | 15110 | 1087 | 15331 | 1226 | 14368 | 1065 | 327 | 33 | 9.6 | 1.1 | 1.719 | 0.000 | 86 | 6 | 0.29 | 0.061 |
| 6c | 7.44 | 0.01 | 18640 | 1395 | 18416 | 1372 | 17432 | 1296 | 546 | 50 | 12.8 | 1.7 | 1.715 | 0.000 | 114 | 2 | 0.31 | 0.062 |
| 6d | 7.49 | 0.02 | 22684 | 1084 | 16951 | 639 | 16018 | 600 | 577 | 45 | 14.1 | 1.5 | 1.715 | 0.000 | 130 | 7 | 0.42 | 0.078 |
| 6e | 7.46 | 0.01 | 31275 | 1792 | 26396 | 1744 | 24973 | 1648 | 829 | 64 | 17.5 | 2.4 | 1.703 | 0.000 | 120 | 2 | 0.26 | 0.062 |
| 6f | 8.38 | 0.01 | 5348 | 42 | 4324 | 32 | 3446 | 27 | 868 | 13 | 11.2 | 0.6 | 0.402 | 0.000 | 150 | 2 | 0.40 | 0.079 |
| 6g | 8.24 | 0.00 | 10397 | 146 | 8952 | 136 | 7573 | 125 | 1348 | 14 | 17.2 | 0.8 | 0.397 | 0.000 | 119 | 1 | 0.23 | 0.073 |
| 6h | 7.91 | 0.01 | 7949 | 104 | 7033 | 92 | 6139 | 85 | 852 | 24 | 12.7 | 0.6 | 0.399 | 0.000 | 90 | 2 | 0.23 | 0.073 |
| 7g | 8.00 | 0.00 | 20209 | 219 | 18509 | 211 | 16657 | 199 | 1733 | 18 | 23.6 | 0.9 | 0.399 | 0.000 | 79 | 1 | 0.14 | 0.072 |
| 7h | 8.01 | 0.01 | 10056 | 110 | 8919 | 110 | 7793 | 108 | 1078 | 14 | 15.3 | 0.6 | 0.397 | 0.000 | 94 | 1 | 0.23 | 0.082 |
| 8f | 7.90 | 0.03 | 8138 | 409 | 7545 | 363 | 6897 | 321 | 585 | 57 | 12.7 | 1.4 | 0.396 | 0.000 | 66 | 4 | 0.21 | 0.076 |
| 8g | 8.49 | 0.01 | 10083 | 143 | 7974 | 114 | 6028 | 87 | 1932 | 34 | 25.8 | 1.3 | 0.397 | 0.000 | 172 | 1 | 0.22 | 0.057 |
| 8h | 8.28 | 0.00 | 13102 | 185 | 11418 | 168 | 9777 | 149 | 1600 | 19 | 20.1 | 0.9 | 0.399 | 0.000 | 116 | 1 | 0.22 | 0.076 |
| 9g | 7.79 | 0.01 | 30772 | 528 | 29287 | 503 | 27224 | 468 | 1746 | 42 | 21.9 | 1.4 | 0.402 | 0.000 | 53 | 1 | 0.09 | 0.071 |
| 9h | 7.89 | 0.01 | 16954 | 402 | 15830 | 385 | 14510 | 360 | 1187 | 27 | 14.1 | 1.1 | 0.402 | 0.000 | 65 | 1 | 0.14 | 0.075 |
| 10g | 8.09 | 0.01 | 15660 | 461 | 14071 | 428 | 12436 | 390 | 1562 | 41 | 18.3 | 1.6 | 0.398 | 0.000 | 92 | 1 | 0.20 | 0.087 |
| 10h | 7.78 | 0.01 | 29597 | 532 | 28033 | 485 | 26074 | 441 | 1648 | 61 | 21.0 | 1.6 | 1.716 | 0.017 | 223 | 6 | 0.30 | 0.055 |
| 11g | 7.80 | 0.01 | 23314 | 436 | 21955 | 419 | 20382 | 395 | 1343 | 26 | 17.3 | 1.1 | 1.790 | 0.028 | 242 | 4 | 0.39 | 0.060 |

| | | | | | | | | | | | | | | | | | | |
|---|---|---|---|---|---|---|---|---|---|---|---|---|---|---|---|---|---|---|
| 12g | 8.87 | 0.03 | 6744 | 306 | 4489 | 145 | 2530 | 10 | 1956 | 150 | 24.1 | 3.6 | 0.398 | 0.000 | 256 | 7 | 0.38 | 0.065 |
| 13g | 7.90 | 0.01 | 8296 | 392 | 7711 | 363 | 7069 | 329 | 579 | 34 | 10.6 | 0.9 | 0.396 | 0.000 | 65 | 1 | 0.19 | 0.069 |
| 13h | 9.32 | 0.01 | 5177 | 382 | 2809 | 227 | 895 | 72 | 1913 | 156 | 24.9 | 3.3 | 0.394 | 0.000 | 329 | 1 | 0.57 | 0.073 |

Table S3. Pearson correlation coefficients for mean solution chemistry parameters showing the most significant correlations with the B/Ca ratio of the precipitate, as well as various proposed ratios suggested to be linked to B/Ca regardless of significance. Correlation coefficients are given for the data set as a whole as calculated in the main text (Table 1), for calculations using the Pitzer model of Hain et al. (2015), and for calculations using the Pitzer model of Hain et al. (2015) taking into account the effects of [Mg] and [Ca].

| Species in solution | Correlation with B/Ca (main text) | Correlation with B/Ca (Pitzer model) | Correlation with B/Ca (correcting for [Mg] and [Ca]) |
|---|---|---|---|
| $pH_T$ | 0.03 | 0.03 | 0.03 |
| $[HCO3^-]$ | -0.16 | -0.16 | -0.18 |
| DIC | -0.18 | -0.17 | -0.18 |
| $[B(OH)_4^-]^2 /[CO_2][HCO_3^-]^2$ | 0.19 | 0.19 | 0.19 |
| $[B(OH)_4^-]/[HCO_3^-]$ | 0.33 | 0.32 | 0.35 |
| $[B(OH)_4^-]/([CO_3^{2-}] + [HCO_3^-])$ | 0.47 | 0.47 | 0.51 |
| $[B(OH)_3]$ | 0.55 | 0.55 | 0.55 |
| $[B(OH)_4^-]$ | 0.79 | 0.78 | 0.84 |

| | | | |
|---|---|---|---|
| $[B]/[HCO_3^-]$ | 0.81 | 0.79 | 0.83 |
| $[B(OH)_4^-]/[CO_3^{2-}]$ | 0.83 | 0.83 | 0.86 |
| $[B]/([CO_3^{2-}] + [HCO_3^-])$ | 0.89 | 0.89 | 0.89 |
| [B]/[DIC] | 0.89 | 0.89 | 0.89 |
| $[B(OH)_4^-]*[Ca^{2+}]$ | 0.92 | 0.92 | 0.91 |
| $[B(OH)_4^-]/[CO_3^{2-}]^{0.5}$ | 0.95 | 0.95 | 0.95 |

Table S4. Apparent partition coefficients for potential relationships between B/Ca in the precipitate and solution chemistry parameters. Solution chemistry was calculated using constants from Hain et al. (2015) taking into account the effects of [Mg] and [Ca]. B/Ca is in mmol/mol, units are μmol/kg for all solution chemistry parameters except $[Ca^{2+}]$ which is in mmol/kg.

| | $K = B/Ca/[B(OH)_4^-]/[CO_3^{2-}]^{0.5}$ | K = B/Ca/[B]/[DIC] | $K = B/Ca/[B(OH)_4^-]*[Ca^{2+}]$ | $K = B/Ca/[B(OH)_4^-]$ |
|---|---|---|---|---|
| average K | 0.0748 | 4.16 | 0.000227 | 0.00237 |
| minimum K | 0.0455 | 1.59 | 0.000123 | 0.00108 |
| maximum K | 0.111 | 7.12 | 0.000359 | 0.00388 |
| standard deviation | 0.0123 | 1.11 | 0.0000577 | 0.000645 |

Table S5. Mean absolute differences between measured and calculated B/Ca as calculated with equations S1-S10 relative to the measured value and standard deviation.

| | S1 | S2 | S3 | S4 | S5 | S6 | S7 | S8 | S9 | S10 |
|---|---|---|---|---|---|---|---|---|---|---|
| mean | 0.107 | 0.141 | 0.166 | 0.201 | 0.104 | 0.083 | 0.082 | 0.139 | 0.081 | 0.093 |
| standard deviation | 0.082 | 0.118 | 0.145 | 0.188 | 0.76 | 0.066 | 0.065 | 0.140 | 0.067 | 0.074 |

A supplemental .zip file is available which contains detailed data for each run, XRD patterns and/or Raman spectra for each precipitate, a full summary of precipitation chemistry and precipitate chemistry as determined with different measurement and extraction techniques.